

Distances to Galactic OB-stars: Photometry vs. Parallax

J. MICHAEL SHULL AND CHARLES W. DANFORTH¹

¹*CASA, Dept. of Astrophysical and Planetary Sciences
University of Colorado, 389-UCB, Boulder, CO 80309*

ABSTRACT

For application to surveys of interstellar matter and Galactic structure, we compute new spectrophotometric distances to 139 OB stars frequently used as background targets for UV spectroscopy. Many of these stars have updated spectral types and digital photometry with reddening corrections from the Galactic O-Star (GOS) spectroscopic survey. We compare our new photometric distances to values used in previous *IUE* and *FUSE* surveys and to parallax distances derived from *Gaia*-DR2, after applying a standard (0.03 mas) offset from the quasar celestial reference frame. We find substantial differences between photometric and parallax distances at $d > 1.5$ kpc, with increasing dispersion when parallax errors exceed 8%. Differences from previous surveys arise from new GOS stellar classifications, especially luminosity classes, and from reddening corrections. We apply our methods to two OB associations. For Perseus OB1 (nine O-stars) we find mean distances of 2.47 ± 0.57 kpc (*Gaia* parallax) and 2.99 ± 0.14 kpc (photometric) using a standard grid of absolute magnitudes (Bowen et al. 2008). For 29 O-stars in Car OB1 associated with Trumpler-16, Trumpler-14, Trumpler-15, and Collinder-228 star clusters, we find 2.87 ± 0.73 kpc (*Gaia*) and 2.60 ± 0.28 kpc (photometric). Using an alternative grid of O-star absolute magnitudes (Martins et al. 2005) shifts these photometric distances $\sim 7\%$ closer. Improving the distances to OB-stars will require attention to spectral types, photometry, reddening, binarity, and the grid of absolute magnitudes. We anticipate that future measurements in *Gaia*-DR3 will improve the precision of distances to massive star-forming regions in the Milky Way.

1. INTRODUCTION

Quantitative analyses of the structure of the Milky Way galaxy (Binney & Merrifield 1998) and its interstellar medium (ISM) depend on knowing the distances to stars that map out their positions and motions. These distance estimates began with parallax measurements for local stars and were later extended to photometric distance estimates. Space-astrometric missions (*Hipparcos*, *Gaia*) have expanded the horizon for parallax measurements to stars at kiloparsec scales. Indeed, many astronomers hoped that *Gaia* Data Release 2 (DR2) would provide accurate distances to large numbers of massive OB-type stars throughout the Milky Way (Chan et al. 2019). Similar hopes arose from the Galactic O-Star (GOS) spectroscopic survey (Maíz Apellániz et al. 2004) which generated a large sample of O stars with updated spectral types (Sota et al. 2011, 2014) within several kpc of the Sun. In fact, a systematic discrepancy has appeared between photometric and parallax distances,

as discussed below. The GOS digital photometry and optical-NIR dust extinction (Maíz-Apellániz & Barbá 2018) offer an opportunity to compute new “spectrophotometric distances” using current grids of absolute magnitudes for O-stars (Bowen et al. 2008; Martins et al. 2005) which can be compared to distances from *Gaia*.

In this paper, we compute new photometric distances to a sample of OB-type stars frequently used in UV absorption-line studies of Galactic interstellar gas (H I, H₂, O VI). We focus on 139 OB-type stars used as background targets in our forthcoming *FUSE* survey of interstellar H₂ absorption. The goals of this paper are threefold. First, we calculate new photometric distances (D_{phot}) for these OB stars. Second, we estimate parallax distances (D_{Gaia}) from *Gaia*-DR2, applying a single (0.03 mas) parallax offset from the celestial reference frame of quasars. Third, we compare our photometric distances with previous estimates and with *Gaia* distances. We evaluate the differences between the methods, including a critical literature review of spectral types, luminosity classes, photometry, and reddening of all 139 OB stars. Our new photometric

distances are compared to those in previous UV surveys and to *Gaia*-DR2, identifying outliers in plots of D_{phot} vs. D_{Gaia} . Discrepancies in the ratio, $D_{\text{Gaia}}/D_{\text{phot}}$, may arise from dispersion in the parallax offsets or from incorrect SpTs (and absolute magnitudes). Finally, we apply these methods to two Galactic OB associations, Per OB1 and Car OB1. We investigate whether OB-star photometric distances can be used to define cluster membership and characterize the range of parallax offsets.

Recent analyses of *Gaia*-DR2 (Lindgren et al. 2018; Arenou et al. 2018; Brown et al. 2018) found systematic fluctuations in parallaxes relative to the reference frame of distant quasars. For example, parallax offsets were seen in *Gaia* data toward Cepheids (Riess et al. 2018), eclipsing binaries (Stassun & Torres 2018; Graczyk et al. 2019), red-giant stars in the Kepler field with astero-seismic distances (Zinn et al. 2019), and OB stars in the Carina OB1 Association near η Carinae (Davidson et al. 2018). These offsets are greater toward bright stars ($G_{\text{Gaia}} < 12$), and they appear to depend on stellar color and location on the sky. We adopt a standard zero-point parallax offset, $\varpi_{\text{ZP}} = 0.03$ mas, which we add to the tabulated *Gaia* parallax angle (ϖ). Although some studies have found larger offsets (0.05-0.08 mas) for redder stellar populations, we choose 0.03 mas as the appropriate color match between OB stars and the blue spectra of quasars. A mean offset of 0.03 mas has also been found in a recent study of eclipsing binaries (Graczyk et al. 2019). Because the characterization of parallax offsets remains uncertain, we avoid using more complex statistical corrections (Bailer-Jones et al. 2018). Instead, for each star, we apply a correction to the parallax angle to find a distance $D_{\text{Gaia}} = [\varpi + \varpi_{\text{ZP}}]^{-1}$ and an error range $[D_{\text{min}}, D_{\text{max}}]$ based on the formal tabulated *Gaia* errors, $\varpi \pm \sigma_{\varpi}$. All comparisons between D_{Gaia} and D_{phot} assume that the “true parallax distance” lies between these bounds, with possible discrepancies arising from fluctuations in the parallax offset. Later in this paper, we explore possible dependences of the distance ratio, $D_{\text{Gaia}}/D_{\text{phot}}$, on the relative parallax errors (σ_{ϖ}/ϖ), stellar distance, and SpT.

We have avoided statistical corrections to parallax distances, because of the lack of a physical model to characterize the parallax offsets. In this paper, we compare our photometric distances to offset-corrected *Gaia*-DR2 distances and to two previous sets of photometric distances: an *IUE* interstellar survey of intermediate ions (Savage et al. 2001) and the *FUSE* survey of O VI in the Galactic disk (Bowen et al. 2008). Differences in photometric distances between our new values and these surveys arise primarily from the updated spectral types

and luminosity classes, which can change absolute magnitudes M_V by 0.3–0.6 magnitudes. Section 2 reviews previous absorption-line surveys with OB-star targets. Section 3 describes the sample of OB stars and our techniques for deriving photometric and *Gaia* parallax distances. Of special value in comparing D_{Gaia} to D_{phot} is a subset of 84 of the 139 stars with new classifications of spectral type and luminosity class from the GOS spectroscopic survey; 81 of these 84 stars have reliable *Gaia* parallax distances. For the other stars in our survey, we compute D_{phot} from SpTs and photometric data in the literature. As illustrated in several figures, we find a wide dispersion in the ratio of photometric to parallax distances. In Section 4 we apply our methods to two OB associations (Car OB1 and Per OB1) with potential changes to their historical distances. On average, we find reasonable agreement between our photometric distances and D_{Gaia} , but with considerable scatter in the ratio, particularly for stellar distances $d > 1.5$ kpc and parallax errors greater than 8%. We conclude with suggestions for future applications, should *Gaia* analyses better characterize the parallax offsets. This would allow us to calibrate the stellar classifications and provide more accurate distances to OB associations.

2. INTERSTELLAR SURVEYS TOWARD GALACTIC OB STARS

With their high surface temperatures and far-UV continuum fluxes, massive OB-type stars provide bright UV background sources for absorption-line surveys of Galactic interstellar gas (Spitzer & Jenkins 1975; Savage & Sembach 1996). Exploiting the strong UV resonance lines of many elements, these studies have quantified the gaseous content and spatial extent of the ISM in atomic hydrogen (H I), molecular hydrogen (H₂), and many heavy elements (e.g., C, N, O, Mg, Al, Si, P, S, Cl, Ar, Mn, Fe, Ni) over a range of ionization states. Of particular importance were the far-UV surveys of atomic and molecular hydrogen and of the O VI doublet (1031.926 Å and 1037.627 Å) which identified a phase of hotter shock-heated interstellar gas at temperatures 10^5 K to 10^6 K. Since the beginnings of ultraviolet space astronomy in the late 1960s, astronomers have employed a series of UV satellites with spectroscopic instruments to conduct gaseous abundance surveys using OB-stars as background continuum sources. These satellites included *Copernicus*, *IUE*, *FUSE*, and *Hubble Space Telescope* and measured absorption column densities, $N(\text{cm}^{-2})$, along several hundred stellar sight lines. These column densities were translated to average number densities, $\bar{n} = N/d$, along the sight line to each target star, using estimates of its distance (d).

The distances to these OB stars were usually photometric estimates from their apparent visual magnitudes (V), corrected for extinction (A_V) and referenced to absolute magnitudes (M_V) inferred from the spectral type and luminosity class of the star. As we discuss later, photometric distances come with considerable uncertainty, arising from errors in stellar photometry and extinction and from possible stellar mis-classification which affects absolute magnitudes. Distances to the massive O-type stars are required to determine the luminosity density and ionizing photon fluxes in the Galactic disk and low halo (Dove & Shull 1994; Vacca et al. 1996). Distances are also needed to compute the stellar luminosity, correlate the absorption with intervening gas and dust, and place the OB associations into the context of Galactic structure, spiral arms, and molecular clouds. For example, from the Galactic latitude (b) of the stars and their distance above the disk plane, $z = d \sin b$, one can model the vertical scale height of the gas layers (Savage et al. 1977; Shull & Van Steenberg 1985; Diplas & Savage 1994b; Bowen et al. 2008).

The Galactic ISM was first surveyed in the Ly α absorption line of atomic hydrogen by the OAO-2 satellite toward 69 stars of spectral type B2 and earlier, at average distances of 300 pc from the Sun (Savage & Jenkins 1972). The OAO-2 survey was later extended to 95 hot stars (Jenkins & Savage 1974) and the *Copernicus* OAO-3 satellite measured Ly α absorption toward 100 OB stars within 1-2 kpc (Bohlin et al. 1978). The *International Ultraviolet Explorer* (*IUE*) was used for surveys of H I toward 205 OB stars out to 5 kpc (Shull & Van Steenberg 1985) and toward 554 hot stars with heliocentric distances up to 11 kpc (Diplas & Savage 1994a). The latter survey was reduced to a working sample of 393 OB stars (Diplas & Savage 1994b) after excluding B1.5 and B2 stars contaminated by stellar Ly α absorption. Interstellar molecular hydrogen (H_2) was surveyed in its lowest ($J = 0$ and 1) rotational states of the far-UV Lyman and Werner bands using data toward 109 OB-stars with *Copernicus* (Savage et al. 1977). Two decades later, the *Far Ultraviolet Spectroscopic Explorer* (*FUSE*) measured interstellar H_2 absorption toward hot OB-type stars and quasars (Shull et al. 2000; Browning et al. 2003). *FUSE* also surveyed H_2 along 38 translucent lines of sight to OB stars with visual extinction $A_V = 1.0 - 1.5$ (Rachford et al. 2002, 2009) and toward 70 OB stars in the Large and Small Magellanic Clouds (Tumlinson et al. 2002). Ultraviolet satellites also conducted surveys of heavy elements, including studies of C I with *Copernicus* (Jenkins et al. 1983) and the Space Telescope Imaging Spectrograph (STIS) on the *Hubble Space Telescope* (Jenkins & Tripp 2001, 2011). The *IUE*

surveyed low ionization states of Si II, Mg II, Fe II, S II, and Zn II (Van Steenberg & Shull 1988) and intermediate ions Al III, C IV, Si IV (Savage et al. 2001). The highly ionized ISM phase was studied in O VI, first with *Copernicus* (Jenkins & Meloy 1974) and later with *FUSE* (Bowen et al. 2008). For our photometric distance calculations, we employ two grids of absolute magnitudes: our standard OB-star grid from Bowen et al. (2008) and an alternative O-star grid from Martins et al. (2005).

3. DISTANCES FROM PARALLAXES AND PHOTOMETRY

3.1. The Stellar Sample

The 139 OB-type stars chosen for our current study served as UV-background sources for *FUSE* observations of H_2 absorption in the diffuse ISM. A survey of H_2 column densities in various rotational states of the ground vibrational state (J. M. Shull et al. 2019, in preparation) uses these OB stars as bright targets ($V < 10$) with typical color excesses $E(B - V) < 0.5$. To update photometric distances to these stars, we have conducted an extensive review of the literature for SpTs and photometry: B and V magnitudes. The color excess $E(B - V)$ was derived from $(B - V)$ relative to intrinsic colors $(B - V)_0$, and visual extinction followed from $A_V = R_V E(B - V)$, using a standard value ($R_V = 3.1$) for the ratio of total-to-selective extinction. In Section 4.1, where we analyze distances to 29 O-type stars in the Carina Nebula, we adopt a higher value, $R_V = 4.0$, observed by Feinstein et al. (1973) and Tapia et al. (2003) and confirmed here by comparing A_V to $E(B - V)$ for these stars.

Table 1 gives the star names, along with internal ID numbers, Galactic coordinates, spectral types (SpT), and values of B , V , $E(B - V)$, and A_V . Papers that we used for SpT and photometry include classic studies by Morgan et al. (1955), Hiltner (1956), Hiltner & Johnson (1956), Lesh (1968); Schild et al. (1969); Hill (1970), Hill et al. (1974), Garrison et al. (1977), Wesselius et al. 1982, and Schild et al. (1983). A full list of references is provided in footnote (b) of Table 2. A valuable subsample of our 139 stars comes from 84 O-type stars with new spectral classifications from the GOS spectroscopic survey. The main goals of GOS were to obtain high-S/N, moderate-resolution ($R \sim 2500$) blue-ultraviolet spectra of over 1000 O-type stars in the Milky Way and to derive spectral types classified according to well-defined standards (Walborn et al. 2010; Maíz Apellániz et al. 2011). The GOS survey provides both photometry and stellar classification. In our Table 1, we use values ($V_{J,0}$ and $A_{V,J}$) from Maíz Apellániz & Barbá (2018) who mod-

eled optical and NIR photometry with their new family of extinction laws (Maíz Apellániz et al. 2014).

3.2. *Gaia* Parallax Distances

We began our survey by obtaining the basic stellar data of parallaxes and quoted errors (in milli-arcsec) from the on-line *Gaia*-DR2 archive. The catalogue was queried on the *Gaia* archive at the website <http://gea.esac.esa.int/archive>. As recommended by the *Gaia* Mission Team (Lindgren et al. 2018; Arenou et al. 2018) we have applied a constant parallax offset of 0.03 mas to these values, relative to the International Celestial Reference Frame (ICRF) provided by a half-million quasars with accurate VLBI positions (Mignard et al. 2018). The recent astronomical literature contains analyses of parallax offsets ranging from 0.029–0.081 mas for different stellar types (Cepheids, eclipsing binaries, red giants). Riess et al. (2018) determined a 0.046 mas mean offset ($46 \pm 13 \mu\text{as}$) from their *HST* sample of 50 Milky Way Cepheids, and they noted the apparent dependence of the offset on stellar magnitude, color, and position on the sky (Lindgren et al. 2018). Stassun & Torres (2018) found a mean offset of 0.082 mas ($82 \pm 33 \mu\text{as}$) for 89 eclipsing binaries. However, a more recent study (Graczyk et al. 2019) of 81 detached eclipsing binaries found a lower mean offset, 0.031 ± 0.011 mas, in agreement with the value recommended by the *Gaia* team. Zinn et al. (2019) found a mean offset of 0.053 mas (52.8 ± 2.4 [rand] ± 8.6 [syst] μas) using red-giant stars in the *Kepler* field with well-characterized asteroseismic data.

Several recent studies have employed statistical methods (Bailer-Jones et al. 2018; Davies & Beasor 2019) to translate *Gaia* parallax angles and their error range to the most-probable distance. These studies emphasize the need to control for distance bias using statistical methods. Because we are studying individual OB stars, in which the source of the offsets is poorly known, we believe such procedures are not well-suited to our survey. We follow a different procedure, using the *Gaia*-DR2 parallax and error, $\varpi \pm \sigma_\varpi$, to find a formal “parallax distance”, $D_{\text{Gaia}} = [\varpi + \varpi_{\text{ZP}}]^{-1}$, and the corresponding error range, after applying a standard zero-point offset $\varpi_{\text{ZP}} = 0.03$ mas. We then compare D_{Gaia} to the photometric distances and examine the differences and their dependence on stellar parameters, stellar distances, and relative parallax errors. Our comparison of parallax distances with photometric distances finds considerable differences when parallax errors are greater than 8%. As noted earlier, we used a standard parallax offset of 0.03 mas, which we believe to be more appropriate for the blue colors of OB stars rather than higher off-

sets (0.05 mas) for red giants. Table 2 lists the offset-corrected *Gaia* parallax distances for 135 of our 139 survey stars, together with the inferred range of distances based on quoted DR2 parallax errors. We could not use *Gaia* data for four stars (#79, #80, #98, #119) owing to negative parallaxes or unacceptably large errors. We do not include possible systematic errors based on the dependence of offsets on brightness, color, or position on the sky. Typical DR2 parallax errors for the best data are ± 0.03 mas, comparable to the 0.03 mas applied offset. For context, a star at 2.5 kpc distance has a parallax of 0.40 mas. Therefore, offsets of 0.03–0.05 mas can produce 8–15% fractional errors at typical 1–3 kpc distances to the OB stars in our survey.

3.3. Photometric Distances

The initial rationale for this paper was a revised set of photometric distances toward the 139 OB stars used as background targets in our *FUSE* survey of interstellar H₂. Many of these stars appeared in previous surveys of interstellar matter. For example, 100 stars are in common with the *IUE* survey of Al III, Si IV, C IV by Savage et al. (2001), and 101 stars are in common with the *FUSE* survey of O VI in the Galactic disk (Bowen et al. 2008). Many of our 139 stars were used in past UV surveys of interstellar H I (Shull & Van Steenberg 1985; Diplas & Savage 1994a,b) and heavy elements (Van Steenberg & Shull 1988; Jenkins 2009). The new photometric distances in this paper were computed from the usual expression,

$$D_{\text{Shull}} = (10 \text{ pc}) \cdot 10^{(V - A_V - M_V)/5}, \quad (1)$$

with absolute magnitudes M_V from the standard grid in Bowen et al. (2008). For all 139 stars in our study, we used critically evaluated photometry and extinction from the literature.

Potentially more accurate photometric distances may be found for 84 of our 139 stars that appear in the GOS spectroscopic survey (Maíz Apellániz et al. 2004). Revised spectral types for these GOS stars were provided by Sota et al. (2011, 2014), and digital stellar photometry and extinction were tabulated by Maíz Apellániz & Barbá (2018). Based on optical and near-infrared photometry, they list the extinction-corrected visual magnitude, $V_{J,0} \equiv V_J - A_{V_J}$, where the visual extinction A_{V_J} was derived from a new family of extinction laws (Maíz Apellániz et al. 2014). We denote the photometric distances for the GOS survey stars by

$$D_{\text{GOS}} = (10 \text{ pc}) \cdot 10^{(V_{J,0} - M_V)/5}. \quad (2)$$

It is important to determine appropriate values of M_V , the star’s absolute magnitude derived from the star’s

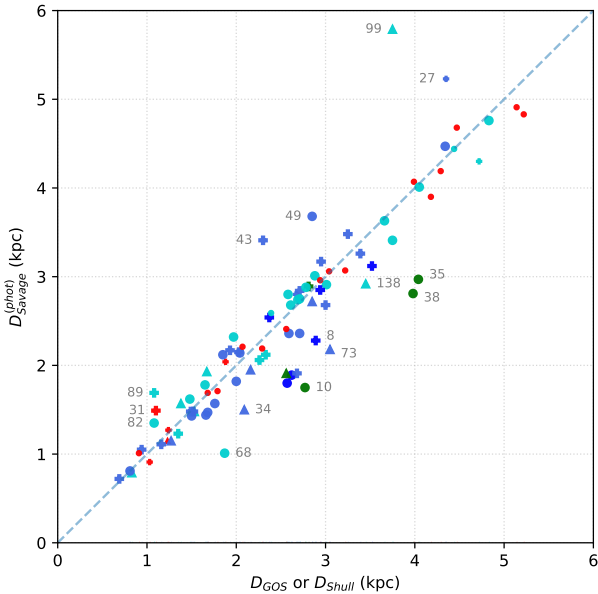


Figure 1. Comparison of our new photometric distances, D_{Shull} or D_{GOS} when available, with D_{Savage} (Savage et al. 2001) for 100 OB stars in common with the *IUE* survey. Outliers are labeled by ID numbers (Tables 1 and 2) and discussed in Appendix A. Neither survey includes error bars, which are primarily systematic (assumptions on SpT and M_V). Stars of similar spectral types are color-coded as follows: dark blue (O2–O4); cornflower blue (O5–O7); cyan = (O8–O9); dark green (ON and WN); red (B0–B4). Luminosity classes are shown as follows: circles (supergiants I, Ia, Iab, Ib, II); triangles (giants II-III, III, III-IV, IV); crosses (main sequence V, IV-V, and unknown).

spectral type (SpT) and luminosity class. Accurate photometric distances require calibration of stellar type (for M_V) as well as visual magnitude V_J and extinction A_{V_J} .

Table 2 lists photometric distances tabulated in two previous ISM surveys, denote as D_{Savage} from the *IUE* survey (Savage et al. 2001) and D_{Bowen} from the *FUSE* survey (Bowen et al. 2008). We also list the offset-corrected parallax distance (D_{Gaia}) and two photometric distance calculations from our current study, denoted D_{Shull} and D_{GOS} (see eqs. [1] and [2]). Figures 1 and 2 compare our new photometric distances with values from previous surveys, D_{Savage} and D_{Bowen} . We find reasonable agreement with D_{Savage} in most cases ($d < 5$ kpc) as seen by the scatter about the one-to-one ratio line. We label 15 outliers on Figure 1, for which the distances differ by more than 15-20%. Deviations from Bowen et al. (2008) are larger (Figure 2) because of differences in photometry (V) and extinction $E(B-V)$. In general, the changes in distance arise from the updated

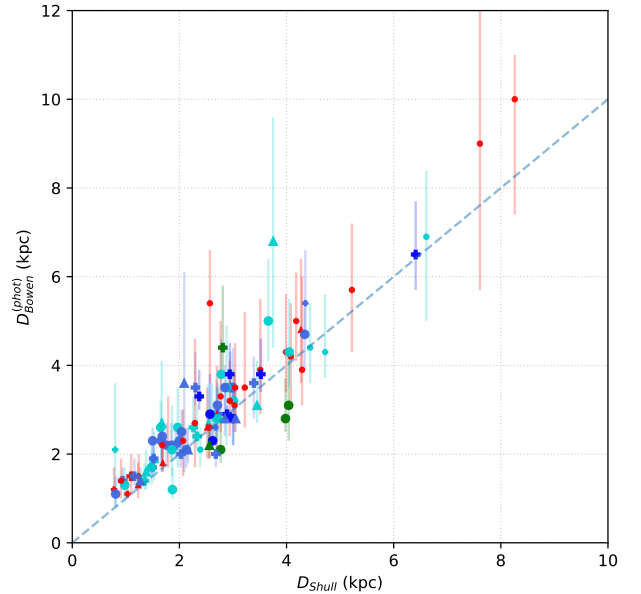


Figure 2. Comparison of new photometric distances, D_{Shull} in Table 2, with 101 OB stars in common with the *FUSE* survey of O VI in Galactic disk (Bowen et al. 2008). Vertical error bars were supplied by Bowen et al. (2008). Color-coding and symbols are the same as in Fig. 1.

spectral types, particularly luminosity classes which can change the absolute magnitudes by $\Delta M_V = 0.3 - 0.6$ magnitudes (factors of 1.15–1.32 in distance). In several cases, changes in the visual extinction contribute to the discrepancies. Appendix A discusses the outliers in Figure 1 and other stars with SpT changes. The subset of 84 GOS stars is particularly useful because their updated stellar classifications and digital photometry provide the extinction-corrected visual magnitude, $V_{J_0} \equiv V_J - A_{V_J}$. The photometric distances labeled D_{GOS} require no assumptions about R_V , provided that one trusts the GOS extinction model (Maíz Apellániz et al. 2014).

Figure 3 compares our photometric distances with *Gaia* distances for 135 stars of the 139 stars. The vertical error bars on D_{Gaia} reflect the internal uncertainties listed in the DR2 database. We have not plotted errors on photometric distances, which are primarily systematic uncertainties in SpT and M_V . Evidently, the *Gaia*-DR2 parallax distances track photometric distances out to distances $d \approx 1.5$ kpc. Increasing scatter and large discrepancies appear at $d > 1.5$ kpc, particularly for early B-stars (red symbols). Within the accuracy of the data, it is difficult to evaluate whether the standard (0.03 mas) parallax offset is any better than higher values (0.05 mas) found for other sources. With the next

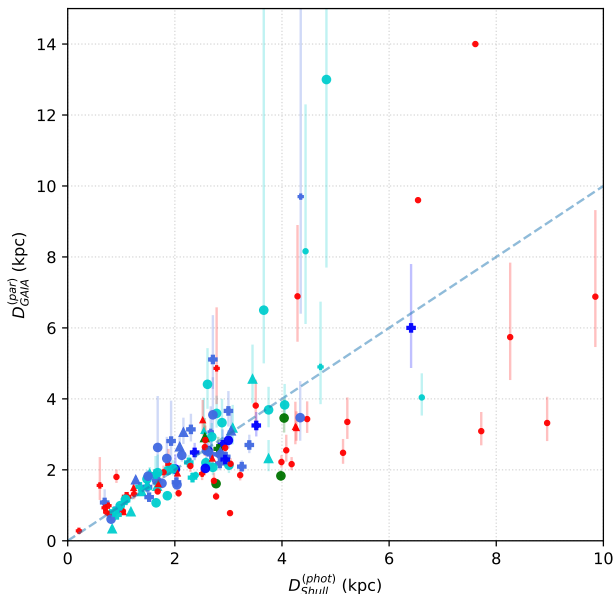


Figure 3. Comparison of new photometric distances, D_{Shull} , with offset-corrected parallax distances (D_{Gaia}) for 135 of the 139 OB stars in our survey. Four stars had missing or unusable *Gaia* data. Color-coding and symbols are as in Fig. 1. Increasingly large discrepancies appear at distances $D > 1.5$ kpc, particularly for the B-type stars (red symbols).

Gaia data release, it may be possible to evaluate the appropriate offset.

Figure 4 provides a similar comparison of D_{Gaia} with photometric distance, D_{GOS} , for the subset of 81 GOS stars with useful parallaxes. In principle, these stars should have more reliable distances, owing to their updated SpTs, digital photometry, and modeled extinction (A_V). However, we continue to see differences between D_{Gaia} and D_{GOS} at $d > 1.5$ kpc. We label the outliers with their ID numbers from Tables 1 and 2 and provide a detailed discussion of the stellar properties and possible reasons for the discrepancies in Appendix A. Four of these stars (#10, #35, #38, #99) also appeared as outliers on Figure 1. In the case of star #99 (HD 168941), our new photometric distance, $D_{\text{GOS}} = 3.72$ kpc, and the parallax distance, $D_{\text{Gaia}} = 2.32$ kpc, are considerably less than previous photometric distances of 6.1 kpc (Tripp et al. 1993) and 5.79 kpc (Savage et al. 2001). The difference hinges on the star’s correct luminosity class (IV vs. II-III).

Figure 5 provides further insight into the Figure 4 outliers. Using data (Table 3) on the parallax angle (ϖ) and its formal error (σ_ϖ) from *Gaia*-DR2 we plot the

parallax-to-photometric distance ratio, $D_{\text{Gaia}}/D_{\text{GOS}}$, versus (ϖ/σ_ϖ) , an indicator of parallax quality. Although most of the GOS stars lie within $\pm 30\%$ of the line of equality, 20 outliers with $D_{\text{Gaia}} > 1.3D_{\text{GOS}}$ (top-left corner) have parallax errors exceeding 20%. Six outliers with $D_{\text{Gaia}} < 0.7D_{\text{GOS}}$ (bottom-right corner) have parallax errors less than 10%. These include stars #38, #10, #86, and #127, each discussed in Appendix A. It is surprising that these stars with low parallax errors would differ from the photometric distances. Some of these discrepancies could arise from complications of close binary orbits on parallax measurements. The 20 stars with $D_{\text{Gaia}} > 1.3D_{\text{GOS}}$ have mean *Gaia* magnitudes $\langle G \rangle = 7.42$, similar to the mean of all 81 GOS stars, $\langle G \rangle = 7.55$. Figure 5 suggests that reliable parallax distances require *Gaia* errors less than about 8%.

4. APPLICATION TO TWO OB ASSOCIATIONS

In addition to comparing individual photometric and parallax distances for 139 OB-type stars in our survey, we applied our techniques to associations of stars. From our sample of O-type stars, supplemented by other O-stars in the GOS survey, we used mean values of *Gaia* parallax distances and new photometric distances to estimate distances to two well-known OB associations: Perseus OB1 and Carina OB1. For this comparison, we used two photometric distance estimates, D_{Shull} and D_{GOS} , for selected O-stars. Table 4 shows the results for 29 O-stars in Carina OB1, and Table 5 lists data for 12 O-stars in Perseus OB1. Both OB associations have been studied extensively, but their estimated distances span a wide range with historical disagreements over their connection with nearby (or embedded) star clusters: the famous “Double Cluster” h and χ Persei (Johnson & Morgan 1955; Slesnick et al. 2002) near Per OB1; and the clusters Trumpler 14, Trumpler 16, Trumpler 15, and Collinder 228 in the Carina Nebula (Humphreys 1978; Massey & Johnson 1993).

4.1. Carina OB1 star clusters

Historical controversy exists (Davidson & Humphreys 1997; Walborn 2012) over the distances to Car OB1 and its associated star clusters, Trumpler 14, Trumpler 15, Trumpler 16, Collinder 228. Thé & Vleeming (1971) derived distances of 2.0 kpc (Tr 14) and 2.5 kpc (Tr 16) and suggested a distance of 2.5 ± 0.2 kpc to the η Carinae Nebula. From a small number of O-type stars, Walborn (1973b) found $DM = 12.72$ (Tr 14), 12.11 (Tr 16), and 12.18 (Col 228). He concluded that Tr 16 and Col 228 “form a single, very young complex located at a distance of 2600 pc” and that Tr 14 “is an exceedingly young, compact cluster which may be as distant as

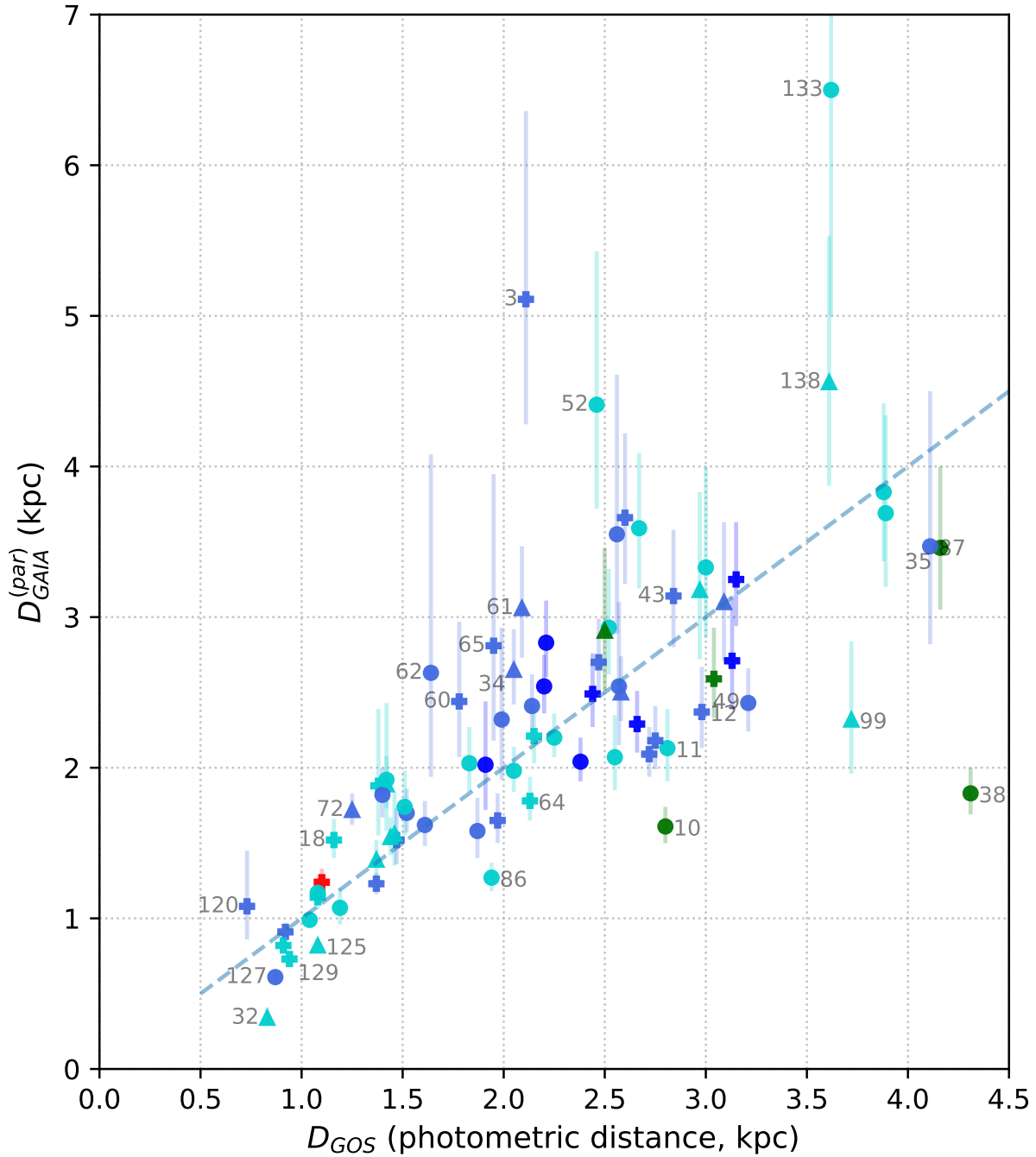


Figure 4. Comparison of *Gaia*-DR2 parallax distances and photometric distances for a subset of 84 O-type stars with new (GOS) stellar classifications (Sota et al. 2011, 2014) and digital photometry (Maíz Apellániz & Barbá 2018). Three of the 84 stars have unusable *Gaia* parallaxes. Outliers are labeled with their ID numbers (Tables 1 and 2). Note the increasing dispersion about the dotted line of equality at distances $d > 1.5$ kpc. More outliers lie above the line ($D_{\text{Gaia}} > D_{\text{GOS}}$) suggesting a broad, asymmetric distribution in parallax offsets. Color-coding and symbols are as in Figure 1. Star #31 with $D_{\text{GOS}} = 1.10$ kpc is labeled with a red cross (for B0.2 V) although it was classified as O9.7 II by GOS; see Appendix A.

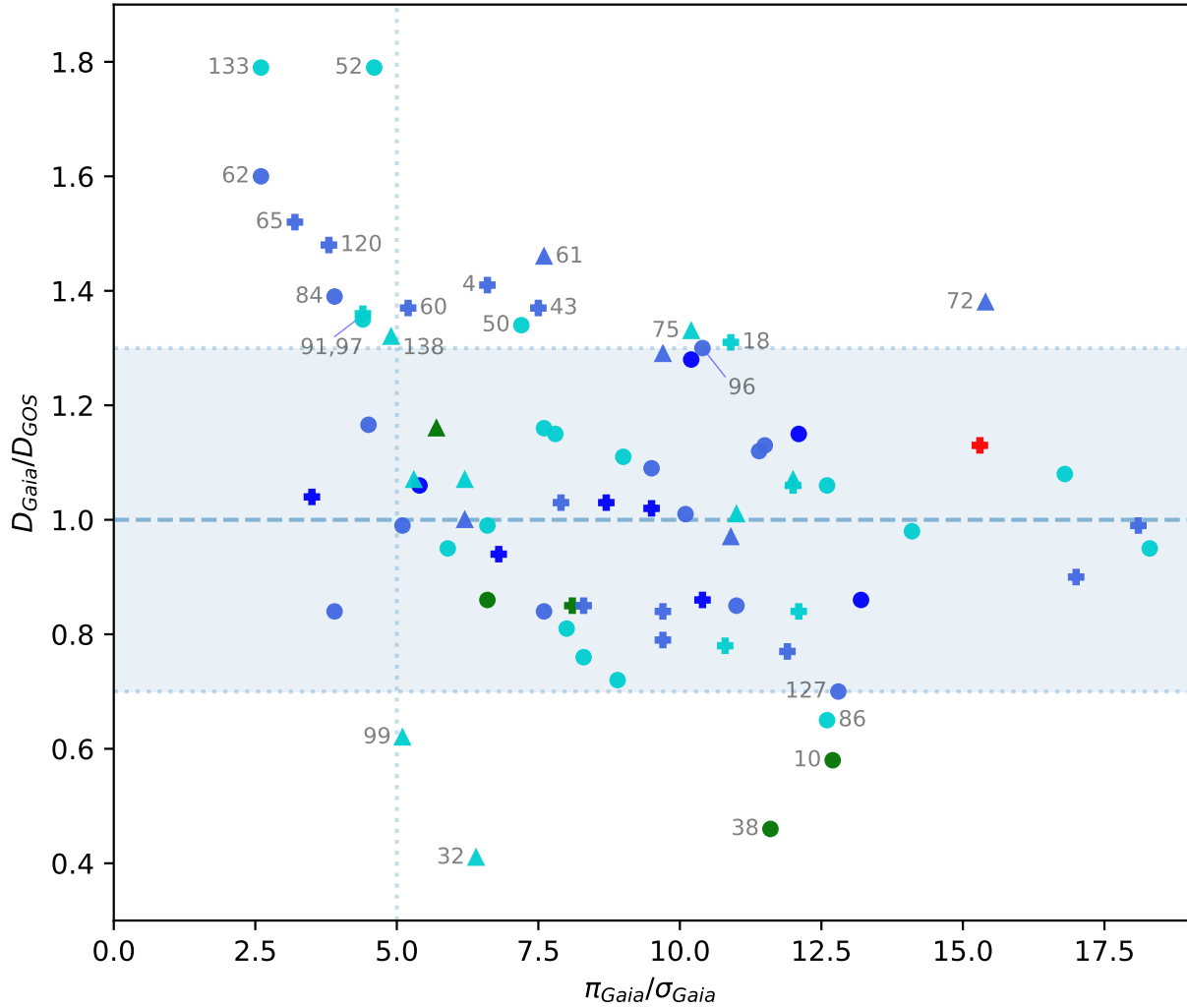


Figure 5. We plot the distance ratio ($D_{\text{Gaia}}/D_{\text{GOS}}$) vs. (ϖ/σ_{ϖ}) , a quality indicator of *Gaia* parallax measurements (see Table 3). Color-coding and symbols are as in Figure 1. Shaded band encloses the boundaries of $\pm 30\%$ deviations from equality, and vertical dotted line at $(\varpi/\sigma_{\varpi}) = 5.0$ marks 20% parallax errors. Of 81 GOS O-type stars with reliable *Gaia* parallaxes, 26 lie outside the $\pm 30\%$ band in an asymmetric distribution: 20 stars have $D_{\text{Gaia}}/D_{\text{GOS}} \geq 1.30$ and 6 stars have $D_{\text{Gaia}}/D_{\text{GOS}} \leq 0.70$. Two stars lie above the top of the plot: Star #3 with $D_{\text{Gaia}}/D_{\text{GOS}} = 2.42$ ($\sigma_{\varpi}/\varpi = 0.23$) and Star #70 with $D_{\text{Gaia}}/D_{\text{GOS}} = 2.66$ ($\sigma_{\varpi}/\varpi = 1.28$). Reasonable distance agreement ($D_{\text{Gaia}} \approx D_{\text{GOS}}$) seems to require parallax errors less than 8%. The outliers, labeled with ID numbers and discussed in Appendix A, may reflect a wide, asymmetric distribution of parallax offsets about the mean value of 0.03 mas. Some of the discrepancies may be produced by binary effects or incorrect luminosity classes (GOS spectroscopic survey).

3500 pc”. After considering age differences of the clusters, Walborn (1982) later revised these distances to a common value, $DM = 12.26 \pm 0.12$ (2.83 ± 0.16 kpc). Feinstein et al. (1973) estimated $DM = 12.65 \pm 0.20$ (3390 ± 300 pc) assuming that Tr 14 and Tr 16 form a common group. Initially adopting $R_V = 3.0$, they corrected the distance to 2650 pc with $R_V \approx 4.0$ because the $(V-I, B-V)$ array indicated anomalous extinction. They also noted a close relationship between the emission nebula, dust, and stars in the cluster. Humphreys (1978) adopted a distance modulus $DM = 12.7$ (3.5 kpc) for Tr 14 and $DM = 12.1$ (2.6 kpc) for Tr 16, assuming $R_V = 3.0$. Using near-infrared (JHKL) photometry, Tapia et al. (1988) adopted $D = 2.4 \pm 0.2$ kpc, for Tr 14, Tr 15, Tr 16, and Coll 228. Massey & Johnson (1993) found $DM = 12.55 \pm 0.08$ (3.2 kpc) for early-type stars in Tr 14 and Tr 16 with $R_V = 3.2$.

Many of the differences in these photometric distances arise from the adopted extinction law and the choice of $R_V = A_V/E(B-V) = 3.0, 3.2, \text{ or } 4.0$. Evidence of anomalous extinction in Carina ($R_V = 4.0$) was first suggested by Feinstein et al. (1973). From their *UBVI* CCD photometry, Hur et al. (2012) also found abnormal reddening with $R_V = 4.4 \pm 0.2$ for stars in the η Carinae Nebula and concluded that Tr 14 and Tr 16 have practically the same $DM = 12.3 \pm 0.2$ (2.9 ± 0.3 kpc). Tapia et al. (2003) carried out large-scale imaging (*UBVR1JHK*) of the Carina Nebula and found $DM = 12.14 \pm 0.67$, with large scatter in both A_V and distance. For the individual clusters, they found mean distance moduli of 12.23 ± 0.67 (Tr 14) and 12.02 ± 0.57 (Tr 16). The Tr 14 and Tr 16 clusters are now regarded to have similar distances, and associated with the massive, eruptive star η Carinae in Tr 16. Spectroscopic velocities of the ejected filaments of the Homunculus Nebula in η Car, combined with the estimated time of ejection, indicated distances of ~ 2.5 kpc (Hillier & Allen 1992) and 2250 ± 180 pc (Davidson et al. 2001). Davidson & Humphreys (1997) previously estimated the distance to η Car at 2.3 ± 0.2 kpc based on luminosities of O stars in Tr 16 and expansion of the η Car ejecta. Using similar methods, Smith (2006) found $D = 2350 \pm 50$ kpc from proper motions of the Homunculus Nebula. The small error on this distance may not include systematic errors in the geometric assumptions.

In our study, we used data toward 29 O-type stars in the Carina Nebula, located in four star clusters. Our statistical analysis (Table 4) considered 16 stars in Tr 16, nine stars in Tr 14, three stars in Coll 228, and one star in Tr 15. We did not include HD 93206 (QZ Car), a complex double-binary system (ID #46 in Appendix A). We compared three estimates of photometric distance

(columns 8, 9, 10 in Table 4) with *Gaia* parallax distance (column 7). The photometric distances were evaluated in three ways. Distances D_{phot} are based on photometry corrected for extinction, similar to D_{Shull} in Table 2 but with an anomalous extinction law, $R_V = 4.0$, rather than the standard value of $R_V = 3.1$. Distances labeled D_{GOS} adopt values of $V_{J,0}$ and A_V , from Maíz Apellániz & Barbá (2018) and listed in columns 3 and 4 of Table 4. These distances are based on our standard grid of absolute magnitudes (Bowen et al. 2008). Distances labeled D'_{GOS} follow the same procedure with GOS photometry, but employ the M_V grid of Martins et al. (2005). For the four clusters in Car OB1, we find mean distances $\langle D_{\text{GOS}} \rangle$ of 2.55 ± 0.30 kpc (Tr 16), 2.68 ± 0.31 kpc (Tr 14), and 2.58 ± 0.35 kpc (Coll 228). The single O-star in Tr 15 had a distance of 2.76 kpc.

We find no significant difference in distances among the four clusters. For the ensemble of all 29 O-type stars, we find mean photometric distances $\langle D_{\text{GOS}} \rangle = 2.60 \pm 0.28$ kpc (absolute magnitudes of Bowen et al. 2008) and $\langle D'_{\text{GOS}} \rangle = 2.42 \pm 0.29$ kpc (absolute magnitudes of Martins et al. 2005). The mean parallax distance is $\langle D_{\text{Gaia}} \rangle \approx 2.87 \pm 0.73$ kpc. Davidson et al. (2018) suggested that the O3 stars in Carina OB1 provide a special population, because of their young age and likely formation proximity. For Tr 16, they noted four such stars (HD 93205, HD 93250, HD 303308, and MJ 257) whose (uncorrected) *Gaia*-DR2 parallaxes had a small dispersion, $\langle \varpi \rangle = 0.383 \pm 0.017$ mas. After applying a 0.030 mas offset, this corresponds to parallax distance $\langle D_{\text{Gaia}} \rangle = 2.42^{+0.19}_{-0.16}$ kpc. Our survey includes three of these stars (ID #45, #48, and #137 in Table 4) whose updated GOS spectral types are O3.5 V, O4 III, and O4.5 V, respectively.

4.2. Perseus OB1

The two open clusters h and χ Persei (the Double Cluster in Perseus) have appeared in the literature (Garmany & Stencel 1992) with distance moduli ranging from $DM = 11.4\text{--}12.0$ corresponding to 1.9–2.5 kpc. Schild (1967) placed h Persei 350 pc more distant and 5 Myr older than χ Persei, with estimates of 2.15 kpc (h) and 2.50 kpc (χ) and an association of “outer group” stars at intermediate distances. In a CCD *UBV* imaging survey, Slesnick et al. (2002) found nearly identical distance moduli, 11.85 ± 0.05 (2.34 ± 0.05 kpc) for stars near the cluster nuclei. However, they did not resolve the question of whether the double cluster is located at the core of Per OB1. Currie et al. (2010) used photometric and spectroscopic observations of stars in h and χ Persei, finding nearly identical properties and distance moduli 11.80–11.85 (2.29–2.34 kpc). Zhong et al. (2019)

used *Gaia*-DR2 data to suggest filamentary substructure extending 200 pc away from the Double Cluster. Also using *Gaia*-DR2 data on red supergiants, Davies & Beasor (2019) found a distance of $2.25^{+0.16}_{-0.14}$ kpc for χ Persei. Lee & Lim (2008) noted the bulk motions of luminous members of this association away from the Galactic plane and the absence of any giant molecular cloud in its vicinity. They suggested sequential star formation in a shell of molecular gas pushed outward by an expanding superbubble. In fact, the O-stars in Per OB1 are spread over $\sim 6 - 8^\circ$ (Humphreys 1978) corresponding to 250-320 pc and consistent with the dispersion in distances. The early O-type stars are likely to be younger than the supergiants. The latter are spread across several degrees of longitude with a corresponding dispersion in distances.

Using data for 12 O-type stars in Per OB1 with GOS photometry, including six from Table 2 and six others (see Table 5), we compared the new photometric distances (D_{Shull} and D_{GOS}) and the *Gaia* parallax distance (D_{Gaia}). From this list, we excluded three stars: HD 15642 and HD 14442 (discrepant large distances) and HD 14633 (at lower Galactic latitude) which are considered uncertain or unlikely association members (Lee & Lim 2008). For the remaining 9 stars, we found mean distances of $\langle D_{\text{phot}} \rangle = 2.95 \pm 0.23$ kpc, $\langle D_{\text{GOS}} \rangle = 2.99 \pm 0.14$ kpc, and $\langle D_{\text{Gaia}} \rangle = 2.47 \pm 0.57$ kpc. One possible cause of the difference could be that our standard grid of absolute magnitudes (Bowen et al. 2008) is too luminous. Adopting the Martins et al. (2005) grid of M_V , we found a 7% lower mean distance, $\langle D'_{\text{GOS}} \rangle = 2.77 \pm 0.22$ kpc. However, this distance was based on only seven stars whose SpTs could be matched or interpolated on the Martins et al. (2005) grid. Unfortunately, they only list three luminosity classes (V, III, I) with large jumps in M_V for classes II and IV.

5. SUMMARY AND FUTURE DIRECTIONS

With the availability of new O-star spectroscopic surveys, *Gaia*-DR2 parallaxes, and technical advances in modeling stellar atmospheres and evolutionary tracks, it is both appropriate and timely to re-assess basic parameters for the most massive stars in our Galaxy. These include photometric distances, which depend on the absolute magnitudes (M_V) associated with SpT and luminosity class. We have calculated new photometric distances to 139 OB-type stars and compared them to parallax distances from *Gaia*-DR2, applying a standard (0.03 mas) parallax offset from the quasar celestial reference frame. Of special value were 84 stars from the GOS spectroscopic survey (Maíz Apellániz et al. 2004) which generated a large sample of O stars within several

kpc of the Sun with updated spectral types (Sota et al. 2011, 2014), accurate digital photometry, and corrections for optical-NIR dust extinction (Maíz Apellániz & Barbá 2018). We used GOS information for these stars, but also compiled values of critically evaluated photometry from the literature for all 139 stars. The GOS stars are presumed to provide more reliable photometric distances, owing to updated spectral types, digital photometry, and reddening corrections. However, as discussed in Appendix A, we explored possible reasons for the discrepancies between photometric and parallax distances for the outliers on Figures 1, 4, and 5. In most cases, the differences result from changes in SpT and luminosity class. These outliers present an opportunity to assess whether large parallax offsets or incorrect stellar classification explain the differences.

A sizable fraction ($\sim 30\%$) of the stars in Figures 4 and 5 exhibit significant differences between our photometric distances and those derived from *Gaia*, particularly at $d > 1.5$ kpc and when *Gaia* parallax errors exceed 8%. The ratio of photometric-to-parallax distances exhibits increasingly large fluctuations about the unit-ratio line in Figure 4. Figure 5 shows that some but not all of these discrepant stars have large parallax errors ($\sigma_\varpi/\varpi > 0.08$). In addition to possible SpT uncertainties, there are also likely systematic errors in *Gaia*-DR2 parallaxes. Stars above the slope-one line would typically require parallax offsets of +0.1 mas to 0.2 mas to bring outliers into agreement ($D_{\text{Gaia}} \approx D_{\text{GOS}}$). Stars below the dotted line would require comparable *negative* parallax offsets, although there are fewer of such stars. Four of these stars (#10, #38, #86, #99) would require offsets of -0.08 mas to -0.23 mas, instead of the standard +0.03 mas. Alternatively, their updated SpTs from GOS may be incorrect, particularly the luminosity classes. Reconciling these distances will require careful examination of the GOS classifications, together with improved parallax measurements.

We have not listed errors in photometric distances, which arise primarily from systematic uncertainties in photometry (B or V magnitudes), extinction corrections (A_V), and the adopted grid of absolute magnitudes (M_V). For the 84 GOS stars (Figures 4 and 5) the photometry (V_J and A_V) are typically accurate to ± 0.02 magnitudes. Thus, changes in SpT or luminosity class are the primary source of differences in our revised photometric distances compared to previous values (Savage et al. 2001; Bowen et al. 2008). A few discrepancies (Figures 1 and 2) arise from different choices of $E(B - V)$ and from using A_V from the GOS survey. In some of those cases, such as stars in the Carina Nebula, we found evidence for anomalous dust extinction ($R_V \approx 4$).

We now summarize the major results of our survey:

1. We find reasonable agreement in our new photometric distances with prior values (Savage et al. 2001) for many of the 100 OB stars in common. Several outliers labeled on Figure 1 differ by more than 15-20%, primarily because of the new spectral types and luminosity classes, which can change the absolute magnitudes by $\Delta M_V = 0.3 - 0.8$. The agreement with 101 stars in Bowen et al. (2008) is not quite as good (Figure 2) because of differences in the adopted GOS photometry (V , A_V) and SpTs.
2. A subset of 84 GOS stars provided updated stellar classifications and digital photometry, including extinction-corrected visual magnitudes requiring no assumptions about R_V . Direct comparison of D_{GOS} and D_{Gaia} (Figures 4 and 5) illustrates the large dispersion between photometric and parallax distances for OB stars at $d > 1.5$ kpc. Reliable *Gaia* parallax distances appear to require parallax measurements with relative errors (σ_ϖ/ϖ) less than 8%.
3. The *Gaia*-DR2 parallax distances track our photometric distances out to $d \approx 1.5$ kpc, with increasing scatter at greater distances. In the sub-sample of 81 GOS O-stars with reliable *Gaia* parallaxes, $\sim 30\%$ (26 stars) have ratios $D_{\text{Gaia}}/D_{\text{GOS}}$ deviating by $\pm 30\%$ from unity. This may reflect a broad, asymmetric distribution in parallax offsets about the applied standard value of 0.03 mas, as well as possible errors in SpTs (and M_V). With the current *Gaia*-DR2 parallax uncertainties (Figure 5) we are unable to establish whether 0.03 mas is a better mean offset than the higher value (0.05 mas) found for red giants. Future data releases might allow us to make such distinctions.
4. Application of our new photometric-distance techniques to two OB associations resulted in revised estimates of their distances. For nine O-type stars in Per OB1 we found $\langle D_{\text{GOS}} \rangle = 2.99 \pm 0.14$ kpc and $\langle D_{\text{Gaia}} \rangle = 2.47 \pm 0.57$ kpc. For 29 O-type stars in Carina OB1, we found $\langle D_{\text{GOS}} \rangle = 2.60 \pm 0.28$ kpc and $\langle D_{\text{Gaia}} \rangle \approx 2.87 \pm 0.73$ kpc, with no statistical difference in distances to the four embedded star clusters (Tr 16, Tr 14, Tr 15, Coll 228).
5. Our new photometric distances, D_{Shull} and D_{GOS} , are based on a standard grid of absolute magnitudes from Bowen et al. (2008). Changing to the grid of Martins et al. (2005), with lower luminosities for O-type stars, shifts these distance

closer by $\sim 7\%$. For Car OB1, we would then find $\langle D'_{\text{GOS}} \rangle = 2.42 \pm 0.29$ kpc.

From the dispersion of distances shown in Figure 4, it appears that the *Gaia* bright-star error distribution function may have a low-dispersion core and asymmetric high-dispersion wings. Errors in the core correspond to the formal parallax errors, used for our quoted range in D_{Gaia} . For some stars with moderate or large parallax errors ($\sigma_\varpi/\varpi > 8\%$) we see large differences between D_{Gaia} and D_{GOS} . To obtain distance agreement ($D_{\text{Gaia}} \approx D_{\text{GOS}}$) for these outliers, we would need to apply both positive and negative offsets (0.1–0.3 mas) from wings of the error distribution function. As noted above, 26 of 81 GOS stars in Figure 5 have $D_{\text{Gaia}}/D_{\text{GOS}}$ ratios deviating by $\pm 30\%$ from unity. The distribution appears to be asymmetric, with 20 outliers above the 1.3-ratio line, but only 6 stars below the 0.7-ratio line. In determining distances to structures containing many O-type stars, one can sample the low-dispersion core of the error distribution and ignore the outliers, as we did for Car OB1 and Per OB1. Thus, the cluster membership issues suggested for Trumpler 16 (Davidson et al. 2018) may be caused by broad wings in the parallax-offset distribution rather than cluster membership.

These new photometric distances toward OB-type stars will be adopted in our upcoming survey of H_2 from *FUSE* spectra. The techniques developed in this pilot study can be extended to other O-stars in the GOS spectroscopic survey and compared to those used in previous *IUE*, *FUSE*, and *HST* surveys of interstellar matter. For selected OB associations, we can employ main-sequence fitting of well-observed Galactic OB associations to determine a new M_V calibration for OB stars. We can use stars in Sco OB2, and Ori OB1 as local distance anchors. The OB stars in the LMC, with their precise distances and large pool of luminosity class I and III sources, will provide a crucial addition to the sample. Previous studies, as well as recent theoretical stellar atmosphere models (Hainich et al. 2019) have found almost no difference between the M_V -spectral type calibrations between LMC and Galactic OB stars. This should allow us to assess the consistency of absolute magnitude tables (Vacca et al. 1996; Martins et al. 2005; Bowen et al. 2008). These consistency checks should be based on physical constraints, $L = 4\pi R^2 \sigma T_{\text{eff}}^4$ and $g = GM/R^2$ (with rotational corrections) for SpTs with SpT grids from O2 to B2 in all luminosity classes (V, IV, III, II, I). The computed model atmospheres and flux grids may also contain errors comparable to the systematic errors in *Gaia* parallax, arising from stellar rotation, outflows, MHD turbulence, and other physical effects.

The discussion in Appendix A demonstrates that the resolution of outliers in spectroscopic distance comparisons could involve either changes in parallax offsets or modification of the GOS stellar classifications. Tripp et al. (1993) noted that some late O-type and early B-type stars could use UV line diagnostics (Massa 1989) to distinguish the correct luminosity classes. Our new spectroscopic distances may benefit from such updates, in order to obtain better agreement between D_{phot} and D_{Gaia} after the next *Gaia* data release (DR3) currently scheduled for late 2020.

Acknowledgements. This work has made use of data from the European Space Agency (ESA) mission *Gaia* (<https://www.cosmos.esa.int/gaia>), processed

by the *Gaia* Data Processing and Analysis Consortium (DPAC, <https://www.cosmos.esa.int/web/gaia/dpac/consortium>). Funding for the DPAC has been provided by national institutions, in particular the institutions participating in the *Gaia* Multilateral Agreement. We thank Blair Savage, Ed Jenkins, Bill Vacca, Roberta Humphreys, Kris Davidson, and Nathan Smith for helpful discussions on OB stars and the Carinae Nebula. We are also grateful to Jesús Maíz Apellániz for clarifications about the GOS spectroscopic survey and to Jeremy Darling and Joel Zinn for advice about *Gaia* parallax uncertainties.

APPENDIX

A. NOTES ON SPECIFIC STARS

Below, we provide brief discussion of photometric distance estimates for stars labeled as outliers on plots that compare our work to previous photometric distances (Figure 1) or to *Gaia* parallax distances (Figures 4 and 5). Data on *Gaia*-DR2 parallaxes ($\varpi \pm \sigma_\varpi$) are listed in Table 3. We also elaborate on the assumptions made for complex binary systems and uncertain classifications. We are particularly interested in outliers in Figure 5 with distance ratios $D_{\text{Gaia}}/D_{\text{GOS}}$ deviating by $\pm 30\%$ from unity. Are these the result of parallax errors or incorrect spectrophotometric distances? How well are the SpTs classified? How accurate are the absolute magnitudes?

A.1. Outliers on Figure 1

#10 (HD 13268). Our photometric distance estimates, $D_{\text{Shull}} = 2.77$ kpc and $D_{\text{GOS}} = 2.80$ kpc, are larger than previous values, 1.75 kpc and 2.1 kpc from Savage et al. (2001) and Bowen et al. (2008). The difference arises from the GOS spectral type ON8.5 III (Sota et al. 2014) compared to ON8 V (Savage et al. 2001). This produces a change in absolute magnitude $\Delta M_V = -0.80$ (ON8.5 III is more luminous). The *Gaia* distance is 1.61 kpc (range 1.50-1.74 kpc). From the spectrum in Figure 14 of Sota et al. (2014), it is difficult to assess subtle differences between luminosity classes III and V in the diagnostic lines, N III (4634, 4640), C III (4650), He II (4686).

#27 (HD 63005). Our photometric distance estimate, $D_{\text{Shull}} = 4.35$ kpc (no GOS data), is lower than previous values, 5.23 kpc and 5.4 kpc from Savage et al. (2001) and Bowen et al. (2008). We adopted a SpT of O7 V (Markova et al. 2011) compared to O6 V (Savage et al. 2001) who reference Garrison et al. (1977). This produces $\Delta M_V = 0.30$ (O7 V is less luminous). Markova et al. (2011) discuss a range in SpTs from O6.5 V to O7.5 V depending on resolution of the classifying spectrum; we adopt O7 V as a median value.

#31 (HD 69106). Our photometric distance estimates, $D_{\text{Shull}} = 1.12$ kpc and $D_{\text{GOS}} = 1.10$ kpc, are lower than previous values, 1.49 kpc and 1.5 kpc from Savage et al. (2001) and Bowen et al. (2008). Our photometric distances are similar to $D_{\text{Gaia}} = 1.24$ kpc (range 1.17–1.33 kpc). We distrust the SpT of O9.7 II (Sota et al. 2014), as it would imply $M_V = -5.83$ and a photometric distance $D = 2.9$ kpc, much greater than D_{GOS} and D_{Gaia} . Savage et al. (2001) used a SpT of B0.5 IV (Garrison et al. 1977) but we adopt B0.2 V (Markova et al. 2011) with $M_V = -3.70$. The SpT difference produces a change in absolute magnitude $\Delta M_V = 0.50$ (B0.2 V is less luminous than B0.5 IV). The star is a fast rotator, which might influence the SpT.

#34 (HD 74920). Our photometric distance estimates, $D_{\text{Shull}} = 2.09$ kpc and $D_{\text{GOS}} = 2.05$ kpc, differ from previous values, 1.50 kpc and 3.6 kpc from Savage et al. (2001) and Bowen et al. (2008). Parallax gives $D_{\text{Gaia}} = 2.65$ kpc (range 2.42–2.92 kpc). We adopt the GOS SpT of O7.5 IV (Sota et al. 2014) rather than O8 (Savage et al. 2001) who reference Thackeray & Andrews (1974) but quote no luminosity class. Vijapurkar & Drilling (1993) refer to this star as LSS 1148

and they assign it O7 III. Differences in SpT are likely responsible for changes in absolute magnitude, particularly with no luminosity class assigned by either Savage et al. (2001) or Bowen et al. (2008).

#35 (HD 89137). Our photometric distance estimates, $D_{\text{Shull}} = 4.16$ kpc and $D_{\text{GOS}} = 4.04$ kpc, are larger than previous values, 2.97 kpc and 3.1 kpc from Savage et al. (2001) and Bowen et al. (2008). The difference arises from the revised GOS spectral type ON9.7 II (Sota et al. 2014) compared to ON9.7 III (Savage et al. 2001) who reference Garrison et al. (1977). This produces a change in absolute magnitude $\Delta M_V = -0.73$ (ON9.7 II is more luminous).

#38 (HD 91651). Our photometric distance estimates, $D_{\text{Shull}} = 4.31$ kpc and $D_{\text{GOS}} = 3.98$ kpc, are larger than previous values, 2.81 kpc and 2.8 kpc from Savage et al. (2001) and Bowen et al. (2008). The difference arises from the revised GOS spectral type ON9.5 III (Sota et al. 2014) compared to O9 V (Savage et al. 2001) who reference Walborn (1973a). This produces a change in absolute magnitude $\Delta M_V = -0.90$ (ON9.5 III is more luminous). We also note a minor transcription error in Savage et al. (2001), who quoted $V = 8.86$ rather than 8.84 (Schild et al. 1983).

#43 (HD 93146A). Our photometric distance estimates, $D_{\text{Shull}} = 2.84$ kpc and $D_{\text{GOS}} = 2.30$ kpc, are smaller than previous values, 3.41 kpc and 3.5 kpc from Savage et al. (2001) and Bowen et al. (2008). We adopt a SpT of O7 V (Sota et al. 2014) whereas Savage et al. (2001) list O6.5 V. This produces a change in absolute magnitude $\Delta M_V = 0.15$ (O7 V is less luminous). This is a binary system, with HD 93146A (O7 V) and HD 93146B (O9.7 IV). A member of Car OB1 and the Coll 228 cluster, with anomalous reddening ($R_V \approx 4$), this star is likely to lie at 2.3-2.6 kpc (see Section 4.1 and Table 4).

#49 (HD 93843). Our photometric distance estimates, $D_{\text{Shull}} = 3.21$ kpc and $D_{\text{GOS}} = 2.85$ kpc, are smaller than previous values, 3.68 kpc and 3.5 kpc from Savage et al. (2001) and Bowen et al. (2008). Parallax gives $D_{\text{Gaia}} = 2.43$ kpc (range 2.24–2.66 kpc). We adopt a SpT of O5 III (Sota et al. 2014), the same as in Savage et al. (2001). The difference in distances does not arise from the adopted photometry. We adopt $V = 7.30$ (star #472 in Schild et al. 1983) and $E(B - V) = 0.28$. Savage et al. (2001) list $V = 7.34$ from the same reference (likely mis-transcribed). GOS photometry (Maíz Apellániz & Barbá 2018) give $V_J = 7.32$ and $A_V = 1.146$. This sight line has anomalous reddening with $A_V/E(B - V) = 4.1$, which accounts for our lower distance $D_{\text{GOS}} = 2.85$ kpc.

#68 (HD 115071). Our photometric distance estimates, $D_{\text{Shull}} = 2.05$ kpc and $D_{\text{GOS}} = 1.87$ kpc, are much larger than previous values, 1.01 kpc and 1.2 kpc from Savage et al. (2001) and Bowen et al. (2008). The difference arises from the revised GOS spectral type O9.5 III (Sota et al. 2014) compared to B0.5 V (Savage et al. 2001) who reference Garrison et al. (1977). This produces a large change in absolute magnitude $\Delta M_V = -1.65$ (O9.5 III is more luminous). We note that $D_{\text{Gaia}} = 1.98$ kpc (range 1.84–2.14 kpc) is consistent with our photometric distances.

#73 (HD 124979). Our photometric distance estimates, $D_{\text{Shull}} = 3.05$ kpc and $D_{\text{GOS}} = 3.09$ kpc, are larger than previous values, 2.18 kpc and 2.8 kpc from Savage et al. (2001) and Bowen et al. (2008). We assume a SpT of O7.5 IV (Sota et al. 2014) compared to O8 V (Savage et al. 2001) who reference Hill et al. (1974). This produces a change in absolute magnitude $\Delta M_V = -0.56$ (O7.5 IV is more luminous than O8 V).

#89 (HD 164816). Our distance estimates, $D_{\text{Shull}} = 1.13$ kpc and $D_{\text{GOS}} = 1.08$ kpc, are smaller than the value, 1.69 kpc, in Savage et al. (2001). They are comparable to $D_{\text{Gaia}} = 1.14$ kpc (range 1.06–1.24 kpc) based on parallax 0.8442 ± 0.0704 mas (8.3% formal error) and 0.03 mas offset. We adopt a SpT of O9.5 V (Sota et al. 2014) with $M_V = -4.15$ compared to O9.5 III-IV (Savage et al. 2001) with $M_V = -4.94$. This produces a change in absolute magnitude $\Delta M_V = +0.79$ (O9.5 V is less luminous). The difference hinges on the star’s luminosity class (V vs. III-IV).

#99 (HD 168941). Our photometric distance estimates, $D_{\text{Shull}} = 3.75$ kpc and $D_{\text{GOS}} = 3.72$ kpc, are smaller than previous values, 5.79 kpc and 6.8 kpc from Savage et al. (2001) and Bowen et al. (2008). The difference arises from the revised GOS spectral type O9.5 IV (Sota et al. 2014) with $M_V = -4.68$ compared to O9.5 II-III (Savage et al. 2001; Tripp et al. 1993) with $M_V \approx -5.52$. This produces a change in absolute magnitude $\Delta M_V = +0.84$ (O9.5 IV is less luminous). Tripp et al. (1993) used UV lines (Si II, Si III, Si IV, C IV, N IV) as classification diagnostics (Massa 1989) and quoted a distance of 6.1 kpc. *Gaia*-DR2 gives $D_{\text{Gaia}} = 2.32$ kpc range 1.96–2.84 kpc) based on parallax 0.4018 ± 0.0792 (20% formal error). The large difference in spectroscopic distances hinges on the star’s luminosity class (IV vs. II-III).

A.2. Outliers on Figure 4

#3 (CPD 59°2600). Our photometric distance estimates, $D_{\text{Shull}} = 2.71$ kpc and $D_{\text{GOS}} = 2.11$ kpc, are lower than previous values, 2.84 kpc and 2.9 kpc from Savage et al. (2001) and Bowen et al. (2008). The GOS spectral type O6 Vf (Sota et al. 2014) is the same as used in previous studies. Our lower value $D_{\text{GOS}} = 2.11$ kpc is a result of

anomalous extinction in Carina. A member of Car OB1 and the Tr 16 cluster with $R_V \approx 4$, this star probably lies at 2.3–2.6 kpc (see Section 4.1 and Table 4). Our photometric distances are much smaller than $D_{\text{Gaia}} = 5.11$ kpc (range 4.28–6.36 kpc) based on parallax 0.1655 ± 0.0382 mas (23% formal error) and 0.03 mas offset. Increasing the parallax offset to 0.20–0.25 mas would bring the parallax distance into better agreement with the photometric distance of Tr 16 and the one-to-one line ($D_{\text{Gaia}} = D_{\text{GOS}}$).

#10 (HD 13268). Our photometric distance estimates, $D_{\text{Shull}} = 2.77$ kpc and $D_{\text{GOS}} = 2.80$ kpc, are larger than $D_{\text{Gaia}} = 1.61$ kpc (range 1.50–1.74 kpc) based on parallax 0.5906 ± 0.0466 mas (7.9% formal error) and 0.03 mas offset. Increasing the parallax offset to larger values would give worse agreement, as star #10 lies below the one-to-one line. This may be a case for a negative parallax offset (–0.23 mas). Alternatively, the SpT (ON 8.5 III) may be incorrect.

#11 (HD 13745). Our photometric distance estimates, $D_{\text{Shull}} = 2.80$ kpc and $D_{\text{GOS}} = 2.81$ kpc, are larger than $D_{\text{Gaia}} = 2.13$ kpc (range 1.91–2.39 kpc) based on parallax 0.4405 ± 0.0528 mas (12.0% formal error) and 0.03 mas offset. Increasing the parallax offset would give worse agreement, as star #11 lies below the one-to-one line. This may suggest a negative parallax offset (–0.08 mas).

#12 (HD 14434). Our photometric distance estimates, $D_{\text{Shull}} = 2.95$ kpc and $D_{\text{GOS}} = 2.98$ kpc, are somewhat larger than $D_{\text{Gaia}} = 2.37$ kpc (range 2.13–2.67 kpc) based on parallax 0.3912 ± 0.0473 mas (12.1% formal error) and 0.03 mas offset. Increasing the parallax offset to larger values would give worse agreement, as star #12 lies below the one-to-one line. This may be a case for a negative parallax offset (–0.05 mas).

#18 (HD 41161). Our photometric distances, $D_{\text{Shull}} = 1.35$ kpc and $D_{\text{GOS}} = 1.16$ kpc, as well as $D_{\text{Savage}} = 1.23$ kpc are lower than $D_{\text{Gaia}} = 1.52$ kpc (range 1.40–1.66 kpc) based on parallax 0.6284 ± 0.0575 mas (9.2% formal error) with 0.03 mas offset. Increasing the parallax offset to 0.20 mas would bring the star into closer agreement with the one-to-one line.

#32 (HD 73882). Our photometric distance estimates, $D_{\text{Shull}} = 1.00$ kpc and $D_{\text{GOS}} = 0.83$ kpc, are similar to 0.79 kpc (Savage et al. 2001) but much larger than $D_{\text{Gaia}} = 0.34$ kpc (range 0.30–0.41 kpc) based on parallax 2.8856 ± 0.4507 mas (16% formal error) with 0.03 mas offset. Our SpT of O8.5 IV from Sota et al. (2014) differs from O8 V in Savage et al. (2001) who quote Garrison et al. (1977). This produces a change in absolute magnitude $\Delta M_V = -0.32$ (O8.5 IV is more luminous). GOS photometry gives $V_J = 7.25$ (Maíz Apellániz & Barbá 2018) similar to $V = 7.22$ (Savage et al. 2001) who quote Schild et al. (1983). Our derived value $E(B - V) = 0.69$ agrees with Savage et al. (2001). The system is listed as an eclipsing binary, which could affect parallax measurements.

#34 (HD 74920). Our photometric distance estimates, $D_{\text{Shull}} = 2.09$ kpc and $D_{\text{GOS}} = 2.05$ kpc, are smaller than $D_{\text{Gaia}} = 2.65$ kpc (range 2.42–2.92 kpc) based on parallax 0.3479 ± 0.0358 mas (10% formal error) and 0.03 mas offset. Increasing the parallax offset to 0.14 mas would bring the star into closer agreement with the one-to-one line. As noted in Section 6.1, differences in SpT (O7.5 IV vs. O7 III) could produce a sizeable change in absolute magnitude.

#38 (HD 91651). Our photometric distance estimates, $D_{\text{Shull}} = 4.31$ kpc and $D_{\text{GOS}} = 3.98$ kpc, are larger than $D_{\text{Gaia}} = 1.83$ kpc (range 1.69–2.00 kpc) based on parallax 0.5167 ± 0.0455 mas (8.8% formal error) and 0.03 mas offset. Increasing the parallax offset would give worse agreement, as star #38 lies below the one-to-one line. This may be a case for a negative parallax offset (–0.27 mas) or an incorrect SpT (see Section 6.1).

#43 (HD 93146A). Our photometric distance estimates, $D_{\text{Shull}} = 2.84$ kpc and $D_{\text{GOS}} = 2.30$ kpc, are smaller than $D_{\text{Gaia}} = 3.14$ kpc (range 2.80–3.58 kpc) based on parallax 0.2880 ± 0.0386 mas (13.4% formal error) and 0.03 mas offset. A member of Car OB1 and the Coll 228 cluster with anomalous reddening ($R_V \approx 4$), this star is likely to lie at 2.3–2.6 kpc (see Section 4.1 and Table 4). Increasing the parallax offset to 0.10 mas would bring the star into better agreement with the cluster distance and the one-to-one line.

#50 (HD 96670). We find good agreement in all three photometric distances, $D_{\text{Shull}} = 2.78$ kpc, $D_{\text{GOS}} = 2.67$ kpc, and $D_{\text{Savage}} = 2.88$ kpc, all smaller than $D_{\text{Gaia}} = 3.59$ kpc (range 3.18–4.09 kpc) based on parallax 0.2418 ± 0.0344 (14% formal error) and 0.03 mas offset. Increasing the parallax offset to 0.12 mas would bring the star into better agreement with the one-to-one line. This star did not appear with a SpT in the GOS papers (Sota et al. 2011, 2014). We adopted O8 Ibf (Garrison et al. 1977) with GOS photometry from Maíz Apellániz & Barbá (2018).

#52 (HD 96917). We find good agreement in all three photometric distances, $D_{\text{Shull}} = 2.61$ kpc, $D_{\text{GOS}} = 2.46$ kpc, and $D_{\text{Savage}} = 2.68$ kpc, all smaller than $D_{\text{Gaia}} = 4.41$ kpc (range 3.72–5.43 kpc) based on parallax 0.1966 ± 0.0423 (22% formal error) and 0.03 mas offset. Increasing the parallax offset to 0.20 mas would bring the star into agreement with the one-to-one line.

#60 (HD 101131). Our photometric distance estimates, $D_{\text{Shull}} = 2.03$ kpc and $D_{\text{GOS}} = 1.78$ kpc, are similar to previous distances, $D_{\text{Savage}} = 1.91$ kpc and $D_{\text{Bowen}} = 2.0$ kpc. All are smaller than $D_{\text{Gaia}} = 2.44$ kpc (range 2.07–2.97 kpc) based on parallax 0.3795 ± 0.0729 mas (19.2% formal error) and 0.03 mas offset. This star has anomalous reddening ($R_V \approx 4$) based on $A_V = 1.228$ from GOS (Maíz Apellániz & Barbá 2018) and our value $E(B - V) = 0.31$. Increasing the parallax offset to 0.15 mas would bring the star into better agreement with the one-to-one line.

#61 (HD 101190). Our photometric distance estimates, $D_{\text{Shull}} = 2.16$ kpc and $D_{\text{GOS}} = 2.09$ kpc, are similar to $D_{\text{Savage}} = 1.95$ kpc and $D_{\text{Bowen}} = 2.1$ kpc, but considerably smaller than $D_{\text{Gaia}} = 3.06$ kpc (range 2.73–3.47 kpc) based on parallax 0.2971 ± 0.0389 mas (13.1% formal error) and 0.03 mas offset. Increasing the parallax offset to 0.20 mas would bring the star into better agreement with the one-to-one line. The composite spectrum indicates a B-star companion that could affect the parallax measurement.

#62 (HD 101205). Our photometric distance estimates, $D_{\text{Shull}} = 1.68$ kpc and $D_{\text{GOS}} = 1.64$ kpc, are similar to previous distances, $D_{\text{Savage}} = 1.47$ kpc and $D_{\text{Bowen}} = 2.4$ kpc, but smaller than $D_{\text{Gaia}} = 2.63$ kpc (range 1.94–4.08 kpc) based on parallax 0.3557 ± 0.1354 mas (39% formal error) and 0.03 mas offset. Increasing the parallax offset to 0.25 mas would bring the star into better agreement with the one-to-one line.

#64 (HD 101413). Our photometric distance estimates, $D_{\text{Shull}} = 2.33$ kpc and $D_{\text{GOS}} = 2.13$ kpc, are similar to $D_{\text{Savage}} = 2.12$ kpc and $D_{\text{Bowen}} = 2.4$ kpc. They are somewhat larger than $D_{\text{Gaia}} = 1.78$ kpc (range 1.65–1.94 kpc) based on parallax 0.5304 ± 0.0440 mas (8.3% formal error) and 0.03 mas offset. Increasing the parallax offset to larger values would give worse agreement, as star #64 lies below the one-to-one line. This may be a case for a negative parallax offset (–0.06 mas).

#65 (HD 101436). Our photometric distance estimates, $D_{\text{Shull}} = 1.93$ kpc and $D_{\text{GOS}} = 1.85$ kpc, are similar to $D_{\text{Savage}} = 2.17$ kpc and $D_{\text{Bowen}} = 2.2$ kpc, but smaller than $D_{\text{Gaia}} = 2.81$ kpc (range 2.18–3.95 kpc) based on parallax 0.3257 ± 0.1027 mas (32% formal error) and 0.03 mas offset. Increasing the parallax offset to 0.20 mas would bring the star into better agreement with the one-to-one line.

#72 (HD 124314A). Our photometric distance estimates, $D_{\text{Shull}} = 1.27$ kpc and $D_{\text{GOS}} = 1.25$ kpc, are similar to $D_{\text{Savage}} = 1.15$ kpc and slightly lower than $D_{\text{Bowen}} = 1.4$ kpc (range 1.2–1.7 kpc). Our SpT of O6 IV (Sota et al. 2014) is similar to the O6 V adopted by Savage et al. (2001) quoting Walbrn (1973a). The photometric distances are smaller than $D_{\text{Gaia}} = 1.72$ kpc (range 1.62–1.83 kpc) based on parallax 0.5530 ± 0.0360 mas (6.5% formal error) and 0.03 mas offset. Increasing the parallax offset to 0.25 mas would bring the star into better agreement with the one-to-one line. Because this is a multiple-star system (Sota et al. 2014) with HD 124314A separated by 2.5" from a close binary HD 124314BaBb classified as O9.2 IV, the parallax measurements could be affected.

#86 (HD 161807). Our photometric distances, $D_{\text{Shull}} = 1.86$ kpc and $D_{\text{GOS}} = 1.94$ kpc, are similar to $D_{\text{Bowen}} = 2.1$ kpc. This star was not studied by Savage et al. (2001). Our adopted SpT of O9.7 III (Sota et al. 2014) is slightly earlier than the B0 III in Bowen et al. (2008) quoting Garrison et al. (1977). The photometric distances are larger than $D_{\text{Gaia}} = 1.27$ kpc (range 1.18–1.37 kpc) based on parallax 0.7576 ± 0.0602 mas (8.0% formal error) and 0.03 mas offset. Increasing the parallax offset to larger values would give worse agreement, as star #86 lies below the one-to-one line. This may suggest a negative parallax offset (–0.23 mas). This star is listed as an eclipsing binary (Garrison et al. 1983).

#91 (HD 165246). Our photometric distances are $D_{\text{Shull}} = 1.64$ kpc and $D_{\text{GOS}} = 1.38$ kpc. This star was not studied by either Savage et al. (2001) or Bowen et al. (2008). Our adopted SpT of O8 V (Sota et al. 2014) is the same as that of Garrison et al. (1977). The photometric distances are smaller than $D_{\text{Gaia}} = 1.88$ kpc (range 1.55–2.39 kpc) based on parallax 0.5011 ± 0.1131 mas (23% error) and 0.03 mas offset. Increasing the parallax offset to 0.22 mas would bring the star into better agreement with the one-to-one line.

#96 (HD 167771). Our photometric distances, $D_{\text{Shull}} = 1.50$ kpc and $D_{\text{GOS}} = 1.40$ kpc are similar to the value 1.43 kpc (Savage et al. (2001)). Our adopted SpT of O7 III (Sota et al. 2014) is the same as that in Savage et al. (2001) quoting Walborn (1972). The photometric distances are smaller than $D_{\text{Gaia}} = 1.88$ kpc (range 1.55–2.39 kpc) based on parallax 0.5202 ± 0.0498 mas (9.6% error) and 0.03 mas offset. Increasing the parallax offset to 0.19 mas would bring the star into better agreement with the one-to-one line.

#97 (HD 167971). Our photometric distances are $D_{\text{Shull}} = 1.68$ kpc and $D_{\text{GOS}} = 1.42$ kpc. This star was not studied by either Savage et al. (2001) or Bowen et al. (2008). Our adopted SpT of O8 Ia (Sota et al. 2011) is comparable to previous values of O8 f (Hiltner 1956) and O8 Ib (Walborn 1972). The photometric distances are smaller than

$D_{\text{Gaia}} = 1.92$ kpc (range 1.58–2.43 kpc) based on parallax 0.4918 ± 0.1106 mas (22.5% error) and 0.03 mas offset. Increasing the parallax offset to 0.21 mas would bring the star into better agreement with the one-to-one line.

#99 (HD 168941). Our photometric distance estimates, $D_{\text{Shull}} = 3.75$ kpc and $D_{\text{GOS}} = 3.72$ kpc, are smaller than previous values, 5.79 kpc and 6.8 kpc from Savage et al. (2001) and Bowen et al. (2008), owing to an updated SpT (see Section 6.1 above). They are larger than $D_{\text{Gaia}} = 2.32$ kpc (range 1.96–2.84 kpc) based on parallax 0.4018 ± 0.0792 mas (20% formal error). Increasing the parallax offset to larger values would give worse agreement, as star #99 lies below the one-to-one line. This may be a case for a negative parallax offset (−0.13 mas).

#120 (HD 206267). Our photometric distance estimates, $D_{\text{Shull}} = 0.62$ kpc and $D_{\text{GOS}} = 0.73$ kpc, are similar to $D_{\text{Savage}} = 0.72$ kpc, but smaller than $D_{\text{Gaia}} = 1.08$ kpc (range 0.86–1.45 kpc) based on parallax 0.8952 ± 0.2356 mas (26% formal error) and 0.03 mas offset. A very large (0.40 mas) parallax offset would be required to bring the star into agreement with the one-to-one line. This star was not classified in the GOS papers (Sota et al. 2011, 2014). We adopt a SpT of O6 V from Saurin et al. (2012) who associate this star with H II region IC 1396 and the embedded cluster Trumpler 37 at mean distance $d = 800 \pm 60$ pc. Pan et al. (2004) place this star in Cep OB2 and list $V = 5.62$, $E(B - V) = 0.51$, and $d = 750$ pc. Our photometric distance estimates (0.62–0.73 pc) agree with these observations. The GOS photometry (Maíz Apellániz & Barbá 2018) listed $V_J = 5.688$ and $A_V = 1.584$, so that $R_V \approx 3.1$. This star is a spectroscopic binary (O6 V + O9 V) which might affect parallax measurements.

#125 (HD 209339). Our photometric distance estimates, $D_{\text{Shull}} = 1.18$ kpc and $D_{\text{GOS}} = 1.08$ kpc, were based on a SpT of O9.7 IV (Sota et al. 2014). This star was not studied by Savage et al. (2001) or Bowen et al. (2008). Our photometric distances are larger than $D_{\text{Gaia}} = 0.82$ kpc (range 0.80–0.85 kpc) based on parallax 1.1836 ± 0.0303 mas (2.6% formal error) and 0.03 mas offset. Increasing the parallax offset to larger values would give worse agreement, as star #125 lies below the one-to-one line. This may be a case for a negative parallax offset (−0.25 mas).

#127 (HD 210839). The O-supergiant λ Cep has photometric distance estimates, $D_{\text{Shull}} = 0.81$ kpc and $D_{\text{GOS}} = 0.87$ kpc, based on a SpT of O6.5 I(n)fp (Sota et al. 2011) with photometry $V = 5.05$ and $B - V = 0.25$ (Hiltner 1956) in agreement with the GOS digital photometry (Maíz Apellániz & Barbá 2018). We assume intrinsic color $(B - V)_0 = -0.32$ and $E(B - V) = 0.57$, and we adopt a luminosity class Ib ($M_V = -6.25$). Previous studies found distances of 0.81 kpc (Savage et al. 2001) and 1.1 kpc (Bowen et al. 2008) using a slightly earlier SpT of O6 Inf (Walborn 1973a). Bouret et al. (2012) classified λ Cep as O6 I(n)fp and modeled the stellar parameters with $V = 5.05$, $B - V = 0.192$, $E(B - V) = 0.513$, $M_V = -6.43$, and $d = 0.95 \pm 0.10$ kpc. Pan et al. (2004) adopted O6 Iab with $V = 5.09$, $E(B - V) = 0.56$, and $d = 800$ pc for the Cep OB2 association. Gvaramadze & Gualandris (2011) suggest that λ Cep is a runaway star expelled from Cep OB3. Distances estimates to Cep OB3 range from 725 pc (Blauuw et al. 1959) to 870 pc (Humphreys 1978). A detailed study (Simonson 1968) places λ Cep in the Cep OB2 association, whose distance was estimated at $d = 615 \pm 35$ pc (de Zeeuw et al. 1999) although possibly as large as 800 pc. A SpT of O6 Iab would correspond to $M_V = -6.60$, slightly more luminous than $M_V = -6.43_{-0.12}^{+0.11}$ in the model of Bouret et al. (2012). These photometric distances are all larger than $D_{\text{Gaia}} = 0.61$ kpc (range 0.56–0.66 kpc) based on parallax 1.6199 ± 0.1265 mas (7.8% formal error) and 0.03 mas offset. The *Hipparcos* parallax is similar, 1.65 ± 0.22 mas (van Leeuwen 2007). Because star #127 lies below the one-to-one ratio line (Figures 4 and 5), ringing D_{Gaia} into agreement with photometric distances would require a large negative parallax offset (−0.5 mas). Quite possibly, the SpT of O6.5 I and the corresponding M_V need to be re-examined.

#129 (HD 216532). Our photometric distance estimates, $D_{\text{Shull}} = 0.918$ kpc and $D_{\text{GOS}} = 0.944$ kpc, are larger than $D_{\text{Gaia}} = 0.734$ kpc (range 0.719–0.751 kpc) based on parallax 1.3316 ± 0.0299 mas (2.3% formal error) and 0.03 mas offset. Increasing the parallax offset to larger values would give worse agreement, as star #129 lies below the one-to-one line. This may be a case for a negative parallax offset (−0.25 mas), even though the formal parallax errors are small. Reconciling the distances might require shifting the star to a later SpT than O8.5 V (Sota et al. 2011) to produce a fainter absolute magnitude. However, Hiltner (1956), Morgan et al. (1955), and Garrison (1970) all list this star as O8 V, which would worsen the distance discrepancy. Our adopted $E(B - V) = 0.85$ appears normal, with $R_V = 3.03$ based on $A_V = 2.576$ (Maíz Apellániz & Barbá 2018).

#133 (HD 218915), We find excellent agreement in photometric distances, with $D_{\text{Shull}} = 3.66$ kpc, $D_{\text{GOS}} = 3.62$ kpc, and $D_{\text{Savage}} = 3.63$ kpc. The *Gaia* distance of 5.6 kpc (range 5.0–9.4 kpc) is based on parallax 0.1241 ± 0.0472 mas (38% formal error) and 0.03 mas offset. Increasing the offset to 0.15 mas would bring the star into better agreement with the one-to-one line.

#138 (HD 308813). We find agreement in our new photometric distances, $D_{\text{Shull}} = 2.93$ kpc and $D_{\text{GOS}} = 2.66$ kpc, and previous estimates of 2.92 kpc (Savage et al. 2001) and 3.1 kpc (Bowen et al. 2008). The larger *Gaia* distance of 4.56 kpc (range 3.97–5.53 kpc) is based on parallax 0.1894 ± 0.0386 mas (20% formal error) and 0.03 mas offset. Increasing the parallax offset to 0.10 mas would bring the star into better agreement with the one-to-one line.

A.3. Other stars with SpT discrepancies

#8 (HD 5005A). HD 5005 is a quadruple system (A,B,C,D, all O-type stars). Our photometric distances for HD 5005A, $D_{\text{Shull}} = 3.13$ kpc and $D_{\text{GOS}} = 2.89$ kpc, are larger than 2.28 kpc (Savage et al. 2001) and comparable to 2.9 kpc (Bowen et al. 2008). The difference arises from the GOS spectral type O4 V (Sota et al. 2011) compared to O6.5 V (Savage et al. 2001) who reference Walborn (1973a). This produces a change in absolute magnitude $\Delta M_V = -0.60$ (O4 V is more luminous). The GOS distance of 2.89 kpc is consistent with the water-maser distance of $2.82^{+0.26}_{-0.22}$ kpc (Choi et al. 2014) to the star-forming region G123.06-6.50 in the adjoining nebula NGC 281. *Gaia*-DR2 also provides a consistent (offset-corrected) distance $D_{\text{Gaia}} = 2.71$ kpc.

#42 (HD 93129A). This star was classified by Walborn (1982) as O3If* and later as the prototypical O2 If* star (Walborn et al. 2002). This is the most massive star in the core of Trumpler 14, separated by $2.5''$ from HD 93129B (O3.5 V). We analyze HD 93129A, which was resolved into binary components classified by Sota et al. (2014) as O2 If* (HD 93129Aa) and O3 IIIf* (HD 93129Ab). The GOS photometry (Maíz Apellániz & Barbá 2018) includes all 3 stars (Aa, Ab and B) with $V_{J,0} = 4.825$ and $A_V = 2.199$ (see our Table 4). Gruner et al. (2019) combined observations (HST and VLT) with theoretical spectral decomposition to produce separate parameters for each component: HD 93129Aa [$V = 7.65$, $M_V = -6.09$, $E(B - V) = 0.57$] and HD 93129Ab [$V = 8.55$, $M_V = -5.21$, $E(B - V) = 0.57$]. These result in consistent photometric distances, $D_{\text{phot}} = 2.48$ kpc (Aa) and 2.50 kpc (Ab), for an extinction law with $R_V = 3.1$. If we adopted the anomalous extinction ($R_V = 4.0$) proposed for the Carina Nebula, these distances would drop to 1.96 kpc and 1.98 kpc, respectively. In the combined AB-system, these data imply photometric distances $D_{\text{GOS}} = 2.21$ kpc for $M_V = -6.90$ (Bowen et al. 2008) and $D'_{\text{GOS}} = 1.72$ kpc for $M_V = -6.35$ (Martins et al. 2005).

#46 (HD 93206A). The multiple-star system QZ Car (HD 93206AB) is the brightest object in the Collinder 228 star cluster in the southern part of the Carina Nebula and a double (SB1+SB1) binary (Parkin et al. 2011), consisting of system A (O9.7 Ib + b2 v) and system B (O8 III + o9 v). The lower-case letters indicate that these are not true spectral classifications. The GOS spectroscopic survey gives a combined classification of O9.7 Ib (Sota et al. 2014) with $V_{J,0} = 4.206$ and $A_V = 2.106$ (Maíz Apellániz & Barbá 2018) presumably including all 4 stars in HD 93206AB. Our distance estimates, $D_{\text{Shull}} = 2.23$ kpc and $D_{\text{GOS}} = 1.48$ kpc, are based on the Aa component (O9.7Ib) with $V = 6.31$ and $M_V = -6.18$, corrected for the luminosity ratio, $L_2/L_1 = 0.535$ of the two brightest stars (O8 III and O9.5 Ib). This increases the distance by a factor $[1 + (L_2/L_1)]^{1/2} = 1.24$. Our distances are similar to the value (1.78 kpc) from Savage et al. (2001) but lower than the distance (2.3–2.6 kpc) expected if this system lies in the Carina Nebula (see Table 4).

#48 (HD 93250). Our distance estimates, $D_{\text{Shull}} = 2.62$ kpc and $D_{\text{GOS}} = 2.20$ kpc, are comparable to previous values, 1.89 kpc and 2.3 kpc from Savage et al. (2001) and Bowen et al. (2008). Some difference arises from the revised GOS spectral types, O4 III (Sota et al. 2014) or O4 IV (Maíz Apellaniz et al. 2016), compared to O3 V in Savage et al. (2001). Our photometric distances are based on O4 III. They would change if we adopted the anomalous reddening in Carina with $R_V = 4.0$ or selected the Martins et al. (2005) grid of M_V (see discussion in Section 4.1).

#82 (HD 154368). Our distance estimates, $D_{\text{Shull}} = 1.08$ kpc and $D_{\text{GOS}} = 1.08$ kpc, are smaller than the value, 1.35 kpc, in Savage et al. (2001). We adopt a SpT of O9.2 Iab (Sota et al. 2014) with $M_V = -6.546$ compared to O9 Ia (Savage et al. 2001) with $M_V = -7.00$. This produces a change in absolute magnitude $\Delta M_V = 0.454$ (O9.2 Iab is less luminous). The O9 Ia type comes from Hiltner et al. (1969), whereas Garrison et al. (1977) give O9.5 Iab, which has $M_V = -6.54$.

#105 (HD 179406). This B-type star, also known as 20 Aql, was not in the surveys of Savage et al. (2001) or Bowen et al. (2008). There has been some controversy in the literature over its SpT, with luminosity classes ranging from V to II. Lesh (1968) classifies it as B3 V, while Braganca et al. (2012) classified it as B2/3 II, and Buscombe (1962) listed B3 IV. We adopt the latter classification of B3 IV ($M_V = -2.30$) with $B = 5.46$ and $V = 5.34$ from Braganca et al. (2012). From $(B - V)_0 = -0.20$, we then derive $E(B - V) = 0.33$ and a photometric distance $D_{\text{Shull}} = 211$ pc rather than 147 pc for B3 V ($M_V = -1.52$). Both are smaller than $D_{\text{Gaia}} = 280$ pc (range 267-295 pc) based on parallax 3.5374 ± 0.1720 mas (4.9% formal error) and 0.03 mas offset. A spectral type of B2/3 II, with $M_V = -4.50$

and $(B - V)_0 = -0.22$, would imply $E(B - V) = 0.35$ and a photometric distance of 563 pc. In Table 2 we assume B3 IV and list $D_{\text{Shull}} = 0.21$ kpc.

#109 (HD 190429A). Our distance estimates, $D_{\text{Shull}} = 2.57$ kpc and $D_{\text{GOS}} = 2.38$ kpc, differ from previous values, 1.80 kpc and 2.9 kpc from Savage et al. (2001) and Bowen et al. (2008). We assume a SpT of O4 If (Sota et al. 2011), the same as Savage et al. (2001), and we adopt $M_V = -6.29$ for a Ib luminosity class. The difference in distance appears to arise from the assumed photometry, V and $E(B - V)$. The binary companion, HD 190429B (O9.5 II-III) is separated by $1.959''$ from HD 190429A. We adopt $B = 7.20$ and $V = 7.09$ for HD 190429A (Fabricius et al. 2002) with $E(B - V) = 0.43$, whereas Savage et al. (2001) adopt $V = 6.63$ presumably for the combined (A+B) system. Our adopted $V = 7.09$ magnitude is consistent with the GOS photometry, which gives $V = 7.088$ for HD 190429A (Table 8 of Maíz Apellániz et al. 2004) and $V_J = 6.572$ with $A_V = 1.501$ for HD 190429AB (Maíz Apellániz & Barbá 2018). Bouret et al. (2012) analyze HD 190429A and derive a distance 2.45 ± 0.20 kpc based on $B = 7.201$, $V = 7.088$, $E(B - V) = 0.46$, and $M_V = -6.28$.

#117 (HD 201345). Our distance estimates, $D_{\text{Shull}} = 2.56$ kpc and $D_{\text{GOS}} = 2.50$ kpc, are larger than the value, 1.91 kpc, in Savage et al. (2001). We adopt a SpT of ON9.2 IV (Sota et al. 2014) with $M_V = -4.75$ compared to O9 V (Savage et al. 2001) with $M_V = -4.30$. This produces a change in absolute magnitude $\Delta M_V = -0.45$ (ON9.2 IV is more luminous).

REFERENCES

- Alexander, M. J., Hanes, R. J., Povich, M. S., & McSwain, M. V. 2016, *AJ*, 152, 190
- Arenou, F., Luri, X., Babusiaux, C., et al. 2018, *A&A*, 616, A17
- Bailer-Jones, C. A. L., Rybizki, J., Fousneau, M., Mantelet, G., & Andrae, R. 2018, *AJ*, 156, 58
- Bidelman, W. P. 1951, *ApJ*, 113, 304
- Binney, J., & Merrifield, M. 1998, *Galactic Astronomy*, Princeton University Press
- Blaauw, A., Hiltner, W. A., & Johnson, H. L. 1959, *ApJ*, 130, 69
- Bohlin, R. C., Savage, B. D., & Drake, J. F. 1978, *ApJ*, 224, 132
- Bouret, J.-C., Hillier, D. J., Lanz, T., & Fullerton, A. W. 2012, *A&A*, 544, A67
- Bowen, D. V., Jenkins, E. B., Tripp, T. M., et al. 2008, *ApJS*, 176, 59
- Braganca, G. A., Daflon, S., Cunha, K., et al. 2012, *AJ*, 144, 130
- Brown, A. G. A., Vallenari, A., Prusti, T., et al. 2018, *A&A*, 616, 1
- Browning, M. K., Tumlinson, J., & Shull, J. M. 2003, *ApJ*, 582, 810
- Buscombe, W. 1962, *Mt. Stromlo Obs. Mimeogram*, 4, 1B
- Chen, B.-Q., Huang, Y., Hou, L.-G., et al. 2019, *MNRAS*, 487, 1400
- Choi, Y. K., Hachisuka, K., & Reid, M. J. 2014, *ApJ*, 790, 99
- Crampton, D. 1971, *AJ*, 76, 260
- Currie, T., Hernandez, J., Irwin, J., et al. 2010, *ApJS*, 186, 191
- Davidson, K., & Humphreys, R. M. 1997, *ARA&A*, 35, 1
- Davidson, K., Smith, N., Gull, T. R., Ishibashi, K., & Hillier, D. J. 2001, *AJ*, 121, 1569
- Davidson, K., Helmel, G., & Humphreys, R. M. 2018, *RNAAS*, 2, 133 (arXiv:1808.02073)
- Davies, B., & Beasor, E. R. 2019, *MNRAS*, 486, L10
- Deutschman, W. A., Davis, R. T., & Schild, R. E. 1976, *ApJS*, 30, 97
- de Zeeuw, P. T., Hoogerwerf, R., de Bruijne, J. H.J., et al. 1999, *AJ*, 117, 354
- Diplas, A., & Savage, B. D. 1994a, *ApJS*, 93, 211
- Diplas, A., & Savage, B. D. 1994b, *ApJ*, 427, 274
- Dove, J. B., & Shull, J. M. 1994, *ApJ*, 430, 222
- Ducati, J. R. 2002, *Online Data Catalog of Stellar Photometry*, CDS/ADC Collection, 2237
- Fabricius, C., Hog, E., Makarov, V. V., et al. 2002, *A&A*, 384, 180
- Feinstein, A., Morroco, H. G., & Muzzio, J. C. 1973, *A&AS*, 12, 331
- Fernie, J. D. 1983, *ApJS*, 52, 7
- Garmany, C. D., & Stencel, R. 1992, *A&AS*, 94, 211
- Garrison, R. F. 1970, *AJ*, 75, 1001
- Garrison, R. F., Hiltner, W. A., & Schild, R. E. 1977, *ApJS*, 35, 111
- Garrison, R. F., Schild, R. E., & Hiltner, W. A. 1983, *ApJS*, 52, 1
- Graczyk, D., Pietrzynski, G., Gieren, W., et al. 2019, *ApJ*, 872, 85
- Gruner, D., Hainich, R., Sander, A. A. C., et al. 2019, *A&A*, 621, A63
- Guetter, H. H. 1974, *PASP*, 86, 795
- Gvaramadze, V. V., & Gualandris, A. 2011, *MNRAS*, 410, 304
- Hainich, R., Ramachandran, V., Shenar, T., et al. 2019, et al. 2019, *A&A*, 621, A85
- Hill, P. W. 1970, *MNRAS*, 150, 23
- Hill, P. W., Kilkenny, D., & van Breda, I. G. 1974, *MNRAS*, 168, 451
- Hill, P. W., & Lynas-Gray, A. E. 1977, *MNRAS*, 180, 691
- Hillenbrand, L. A., Massey, P., Strom, S. E., & Merrill, K. M. 1995, *AJ*, 106, 1906
- Hillier, D. J., & Allen, D. A. 1992, *A&A*, 262, 153
- Hiltner, W. A. 1956, *ApJS*, 2, 389
- Hiltner, W. A., Garrison, R. F., & Schild, R. E. 1969, *ApJ*, 157, 313
- Hiltner, W. A., & Johnson, H. L. 1956, *ApJ*, 124, 367
- Hog, E., Fabricius, C., Markov, V. V., et al. 2000, *A&A*, 355, L27
- Howarth, I. D., Siebert, K. W., Hussain, A. J., et al. 1997, *MNRAS*, 284, 265
- Humphreys, R. M. 1978, *ApJS*, 38, 309
- Hur, H., Sung, H., & Bessell, M. S. 2012, *AJ*, 143, 41
- Jenkins, E. B. 2009, *ApJ*, 700, 1299
- Jenkins, E. B., Jura, M., & Loewenstein, M. 1983, *ApJ*, 270, 88
- Jenkins, E. B., & Meloy, D. A. 1974, *ApJ*, 193, L121
- Jenkins, E. B., & Savage, B. D. 1974, *ApJ*, 187, 243
- Jenkins, E. B., & Tripp, T. 2001, *ApJS*, 137, 297
- Jenkins, E. B., & Tripp, T. 2011, *ApJ*, 734, 65
- Johnson, H. L., & Morgan, W. W. 1955, *ApJ*, 122, 429
- Lee, H.-T., & Lim, J. 2008, *ApJ*, 679, 1352
- Lesh, J. R. 1968, *ApJS*, 17, 371
- Levato, H., & Malaroda, S. 1981, *PASP*, 93, 714
- Lindgren, L., Hernández, J., Bombrun, A., et al. 2018, *A&A*, 616, A2
- Maíz Apellániz, J., & Barbá, R. H. 2018, *A&A*, 613, A9
- Maíz Apellániz, J., Evans, C. J., Barbá, R. H., et al. 2014, *A&A*, 564, A63
- Maíz Apellániz, J., Sota, A., Arias, J. I. et al. 2016, *ApJS*, 224, 4

- Maíz Apellániz, J., Sota, A., Walborn, N. R., et al. 2011, in Highlights of Spanish Astrophysics VI, (Madrid, Proceedings of the IX Scientific Meeting of the Spanish Astronomical Society), eds. M. R. Zapatero Osorio, J. Gorgas, J. Maíz Apellániz, J. R. Pardo, A. Gil de Paz, 467
- Maíz Apellániz, J., Sota, A., Arias, J. I. et al. 2016, *ApJS*, 224, 4
- Maíz Apellániz, J., Walborn, N. R., Galué, H. A., & Wei, L. H. 2004, *ApJS*, 151, 103
- Markova, N., Puls, J., Scuderi, S., Simón-Díaz, S., & Herrero, A. 2011, *A&A*, 530, A11
- Martins, F., Schaerer, D., & Hillier, D. J. 2005, *A&A*, 436, 1049
- Massa, D. 1989, *A&A*, 224, 131
- Massey, P., & Johnson, J. 1993, *AJ*, 105, 980
- MacConnell, D. J., & Bidelman, W. P. 1976, *AJ*, 81, 225
- Mermilliod, J.-C., & Mermilliod, M. 1994, *Catalog of Mean UB*
Data in Stars, (New York: Springer Verlag)
- Mignard, F., Klioner, S. A., Lindegren, J., et al. 2018, *A&A*, 616, A14
- Morgan, W. W., Code, A. D., & Whitford, A. E. 1955, *ApJS*, 2, 41
- Pan, H., Federman, S. R., Cunha, K., Smith, V. V., & Welty, D. E. 2004, *ApJS*, 151, 313
- Parkin, E. R., Broos, P. S., Townsley, L. K., et al. 2011, *ApJS*, 194, 8
- Rachford, B. L., Snow, T. P., Destree, J. D., et al. 2009, *ApJS*, 180, 125
- Rachford, B. L., Snow, T. P., Tumlinson, J. D. et al. 2002, *ApJS*, 577, 221
- Reed, B. C., & Beatty, A. E. 1995, *ApJS*, 97, 189
- Riess, A. G., Casertano, S., Yuan, W., et al. 2018, *ApJ*, 861, 126
- Saurin, T. A., Bica, E., & Bonatta, C. 2012, *MNRAS*, 421, 3206
- Savage, B. D., Bohlin, R. C., Drake, J. F., & Budich, W. 1977, *ApJ*, 216, 291
- Savage, B. D., & Jenkins, E. B. 1972, *ApJ*, 172, 491
- Savage, B. D., Meade, M. R., & Sembach, K. R. 2001, *ApJS*, 136, 631
- Savage, B. D., & Sembach, K. R. 1996, *ARA&A*, 34, 279
- Schild, R. E. 1967, *ApJ*, 148, 449
- Schild, R. E. 1970, *ApJ*, 161, 855
- Schild, R. E., Garrison, R. F., & Hiltner, W. A. 1983, *ApJS*, 51, 321
- Schild, R. E., Hiltner, W. A., & Sanduleak, N. 1969, *ApJ*, 156, 609
- Shull, J. M., Tumlinson, J., Jenkins, E. B., et al. 2000, *ApJ*, 538, L73
- Shull, J. M., & Van Steenberg, M. E. 1985, *ApJ*, 294, 599
- Simonson, S. C. 1968, *ApJ*, 154, 923
- Slesnick, C. L., Hillenbrand, L. A., & Massey, P. 2002, *ApJ*, 576, 880
- Smith, N. 2006, *ApJ*, 644, 1151
- Sota, A., Maíz Apellániz, J., Morrell, N. I., et al. 2014, *ApJS*, 211, 10
- Sota, A., Maíz Apellániz, J., Walborn, N. R., et al. 2011, *ApJS*, 193, 24
- Spitzer, L., & Jenkins, E. B. 1975, *ARA&A*, 13, 133
- Stassun, K. G., & Torres, G. 2018, *ApJ*, 862, 61
- Tapia, M., Roth, M., Marraco, H., & Ruiz, M. T. 1988, *MNRAS*, 232, 661
- Tapia, M., Roth, M., Vázquez, R. A., & Feinstein, A. 2003, *MNRAS*, 339, 44
- Thackeray, A. D., & Andrews, P. J. 1974, *A&AS*, 16, 323
- Thé, P. S., & Vleeming, H. 1971, *A&A*, 14, 120
- Tripp, T. M., Sembach, K. R., & Savage, B. D. 1993, *ApJ*, 415, 652
- Tumlinson, J., Shull, J. M., Rachford, B. L., et al. 2002, *ApJ*, 566, 857
- Vacca W. D., Garmany, C. D., & Shull, J. M. 1996, *ApJ*, 460, 914
- Van Steenberg, M. E., & Shull, J. M. 1988, *ApJ*, 330, 942
- van Leeuwen, F. 2007, *A&A*, 474, 653
- Vijapurkar, J., & Drilling, J. S. 1993, *ApJS*, 89, 293
- Walborn, N. R. 1971, *ApJS*, 23, 257
- Walborn, N. R. 1972, *AJ*, 77, 312
- Walborn, N. R. 1973a, *AJ*, 78, 1067
- Walborn, N. R. 1973b, *ApJ*, 179, 517
- Walborn, N. R. 1982, *ApJ*, 254, L15
- Walborn, N. R. 2012, *The Company Eta Carinae Keeps*, in *Eta Carinae and the Supernova Imposters*, *ASSL*, Springer Publ., 384, 25
- Walborn, N. R., Howarth, I. D., Lennon, D.L., et al. 2002, *AJ*, 123, 2754
- Walborn, N. R., Sota, A., Maíz Apellániz, J., et al. 2010, *ApJ*, 711, L143
- Wesselius, P. R., van Duinen, R.J., de Jonge, A. R. W., et al. 1982, *A&AS*, 49, 427
- Zhong, J., Chen, L., Kouwenhoven, M. B. N., et al. 2019, *A&A*, 624, A34
- Zinn, J. C., Pinsonneault, M. H., Huber, D., & Stello, D. 2019, *ApJ*, 878, 136
- Zsargo, J., Fullerton, A. W., Lehner, N., & Massa, D. 2003, *A&A*, 405, 1043

Table 1. Stellar Parameters and Photometry^a

ID	Target	ℓ (deg)	b (deg)	B (mag)	V (mag)	$E(B - V)$ (mag)	SpT	GOS (V_J, A_{V_J})
1	BD 35° 4258	77.19	-4.74	9.42	9.41	0.31	B0.5 Vn	
2	BD 53° 2820	101.24	-1.69	10.05	9.95	0.40	B0 IVn	
3	CPD-59° 2600	287.60	-0.74	8.82	8.61	0.53	O6 Vf	(8.62, 2.19)
4	CPD-59° 2603	287.59	-0.69	8.91	8.77	0.46	O7 Vnz	(8.78, 1.61)
5	CPD-69° 1743	303.71	-7.35	9.40	9.38	0.30	B0.5 IIIIn	
6	CPD-72° 1184	299.15	-10.94	10.61	10.68	0.23	B0 III	
7	HD 3827	120.79	-23.23	7.76	8.01	0.02	B0.7 V	
8	HD 5005A	123.12	-6.24	8.19	8.10	0.41	O4 Vfc	(8.10, 1.44)
9	HD 12323	132.91	-5.87	8.88	8.90	0.29	ON9.2 V	(8.91, 0.74)
10	HD 13268	133.96	-4.99	8.31	8.18	0.44	ON8.5 IIIIn	(8.18, 1.34)
11	HD 13745	134.58	-4.96	7.99	7.83	0.46	O9.7 IIIn	(7.86, 1.45)
12	HD 14434	135.08	-3.82	8.65	8.49	0.48	O5.5 Vnfp	(8.49, 1.47)
13	HD 15137	137.46	-7.58	7.91	7.86	0.35	O9.5 II-IIIIn	(7.87, 1.01)
14	HD 15558A	134.72	+0.92	8.41	7.91	0.82	O4.5 IIIf	(7.93, 2.67)
15	HD 15642	137.09	-4.73	8.61	8.53	0.38	O9.5 II-IIIIn	(8.54, 1.10)
16	HD 34656	170.04	+0.27	6.81	6.79	0.34	O7.5 IIIf	(6.78, 1.16)
17	HD 39680	194.07	-5.88	8.01	7.99	0.34	O6 Vnep	
18	HD 41161	164.97	+12.89	6.68	6.76	0.23	O8 Vn	(6.76, 0.78)
19	HD 42088	190.04	+0.48	7.62	7.55	0.39	O6 Vfz	(7.55, 1.27)
20	HD 45314	196.96	+1.52	6.79	6.64	0.46	O9 npe	
21	HD 46150	206.31	-2.07	6.89	6.76	0.45	O5 Vf	(6.78, 1.44)
22	HD 47360	207.33	-0.79	8.32	8.19	0.41	B0.5 V	
23	HD 47417	205.35	+0.35	6.98	6.97	0.31	B0 IV	
24	HD 60369	242.68	-4.30	8.14	8.15	0.30	O9 IV	
25	HD 61347	230.60	+3.80	8.60	8.43	0.45	O9 Ib	
26	HD 62866	237.48	+1.80	9.08	9.01	0.35	B0.5 IIIIn	
27	HD 63005	242.50	-0.93	9.08	9.13	0.27	O7 Vf	
28	HD 64568	243.14	+0.71	9.43	9.38	0.37	O3 Vf* z	(9.39, 1.39)
29	HD 66695	245.01	+2.21	9.77	9.78	0.27	B0.5 IV	
30	HD 66788	245.43	+2.05	9.36	9.45	0.22	O8 V	
31	HD 69106	254.52	-1.33	7.03	7.13	0.19	B0.2 V	(7.13, 0.63)
32	HD 73882	260.18	+0.64	7.60	7.22	0.69	O8.5 IV	(7.25, 2.59)
33	HD 74194	264.04	-1.95	7.78	7.57	0.50	O8.5 Ib-II	(7.55, 1.82)
34	HD 74920	265.29	-1.95	7.56	7.53	0.35	O7.5 IVn	(7.53, 1.13)
35	HD 89137	279.69	+4.45	7.91	7.98	0.23	ON9.7 IIIn	(7.98, 0.78)
36	HD 90087	285.16	-2.13	7.74	7.76	0.28	O9.2 III	(7.78, 1.03)
37	HD 91597	286.86	-2.37	9.88	9.84	0.30	B1 IIIIne	
38	HD 91651	286.55	-1.72	8.82	8.84	0.28	ON9.5 IIIIn	(8.85, 1.05)
39	HD 91824	285.70	+0.07	8.07	8.14	0.25	O7 Vfz	(8.16, 0.86)
40	HD 92554	287.60	-2.02	9.56	9.47	0.39	O9.5 IIIn	
41	HD 93028	287.64	-1.19	8.24	8.30	0.24	O9 IV	(8.40, 0.84)
42	HD 93129A ^a	287.41	-0.57	7.51	7.26	0.57	O2 If* + O3 IIIIf*	(7.02, 2.20)
43	HD 93146A ^a	287.67	-1.05	8.48	8.45	0.35	O7 Vfz	(8.44, 1.54)
44	HD 93204	287.57	-0.71	8.57	8.48	0.41	O5.5 V̇f	(8.44, 1.61)
45	HD 93205	287.57	-0.71	7.84	7.76	0.40	O3.5 V	(7.74, 1.54)
46	HD 93206A ^a	287.67	-0.94	6.40	6.31	0.39	O9.7 Ibn	(6.31, 2.11)
47	HD 93222	287.74	-1.02	8.15	8.10	0.37	O7 IIIIf	(8.10, 1.84)
48	HD 93250	287.51	-0.54	7.58	7.41	0.49	O4 IIIIfc	(7.36, 1.85)
49	HD 93843	288.24	-0.90	7.26	7.30	0.28	O5 IIIIf	(7.32, 1.15)
50	HD 96670	290.20	+0.40	7.57	7.43	0.46	O8 Ibf	(7.41, 1.50)
51	HD 96715	290.27	+0.33	8.37	8.27	0.42	O4 Vf	(8.25, 1.41)

Table 1 *continued*

Table 1 (*continued*)

ID	Target	ℓ	b	B	V	$E(B - V)$	SpT	GOS
		(deg)	(deg)	(mag)	(mag)	(mag)		(V_J, A_{V_J})
52	HD 96917	289.28	+3.06	7.15	7.07	0.39	O8.5 Ib	(7.08,1.35)
53	HD 97471	290.36	+1.62	9.55	9.30	0.30	B0 V	
54	HD 97913	290.84	+1.41	8.84	8.80	0.32	B0.5 IVn	
55	HD 99857	294.78	-4.94	7.56	7.45	0.35	B0.5 Ib	
56	HD 99890	291.75	+4.43	8.22	8.26	0.24	B0 IIIIn	
57	HD 100199	293.94	-1.49	8.14	8.14	0.30	B0 IIIIne	
58	HD 100213	294.81	-4.14	8.25	8.22	0.34	O8 Vn	(8.39,1.32)
59	HD 100276	293.31	+0.77	7.20	7.16	0.28	B0.5 Ib	
60	HD 101131	294.78	-1.62	7.14	7.15	0.31	O5.5 Vf	(7.14,1.23)
61	HD 101190	294.78	-1.49	7.31	7.27	0.36	O6 IVf	(7.31,1.23)
62	HD 101205	294.85	-1.65	6.48	6.42	0.38	O7 II:	(6.46,1.27)
63	HD 101298	294.94	-1.69	8.11	8.05	0.38	O6 IVf	(8.07,1.41)
64	HD 101413	295.03	-1.71	8.40	8.35	0.36	O8 V	(8.31,1.27)
65	HD 101436	295.04	-1.71	7.62	7.56	0.38	O6.5 V	(7.58,1.30)
66	HD 103779	296.85	-1.02	7.19	7.20	0.23	B0.5 Iab	
67	HD 104705	297.45	-0.34	7.74	7.76	0.26	B0 Ib	
68	HD 115071	305.76	+0.15	8.15	7.94	0.51	O9.5 III	(7.96,1.79)
69	HD 116781	307.05	-0.07	7.73	7.60	0.43	B0 IIIIne	
70	HD 116852	304.88	-16.13	8.38	8.47	0.22	O8.5 II-IIIIf	(8.48,0.67)
71	HD 118571	308.70	+1.35	8.74	8.76	0.26	B0.5 IVn	
72	HD 124314A	312.67	-0.42	6.85	6.64	0.53	O6 IVnf	(6.65,1.69)
73	HD 124979	316.40	+9.08	8.62	8.53	0.41	O7.5 IVn	(8.54,1.25)
74	HD 148422	329.92	-5.60	8.69	8.60	0.35	B1 Ia	
75	HD 152218	343.53	+1.28	7.78	7.61	0.48	O9 IVn	(7.57,1.61)
76	HD 152233	343.48	+1.22	6.72	6.59	0.45	O6 IIIf	(6.58,1.58)
77	HD 152248	343.46	+1.18	6.25	6.10	0.47	O7 Iabf	(6.04,1.59)
78	HD 152314	343.52	+1.14	8.05	7.86	0.50	O9IV	(7.87,1.88)
79	HD 152623	344.62	+1.61	6.75	6.67	0.40	O7 Vnf	(6.69,1.51)
80	HD 152723	344.81	+1.61	7.31	7.16	0.47	O6.5 III	(7.23,1.60)
81	HD 153426	347.14	+2.38	7.61	7.47	0.45	O8.5 III	(7.47,1.56)
82	HD 154368	349.97	+3.22	6.65	6.13	0.81	O9.2 Iab	(6.13,2.52)
83	HD 156292	345.35	-3.08	7.75	7.49	0.56	O9.7 III	(7.51,1.72)
84	HD 157857	12.97	+13.51	7.95	7.78	0.49	O6.5 IIIf	(7.78,1.64)
85	HD 158661	8.29	+9.05	8.32	8.18	0.38	B0.5 Ib	
86	HD 161807	351.78	-5.85	6.92	6.99	0.23	O9.7 IIIIn	(7.01,0.67)
87	HD 163758	355.36	-6.10	7.35	7.32	0.35	O6.5 Iafp	(7.31,1.19)
88	HD 163892	7.15	+0.62	7.60	7.44	0.46	O9 IVn	(7.44,1.44)
89	HD 164816	6.06	-1.20	7.09	7.08	0.31	O9.5 V	(7.08,1.07)
90	HD 165052	6.12	-1.48	6.96	6.86	0.42	O5.5 Vz	(6.86,1.52)
91	HD 165246	6.40	-1.56	7.80	7.71	0.40	O8 Vn	(7.72,1.61)
92	HD 166546	10.36	-0.92	7.26	7.22	0.34	O9.5 IV	(7.22,1.09)
93	HD 166716	14.85	+1.39	7.87	7.95	0.38	B0 II-III	
94	HD 167402	2.26	-6.39	8.94	8.95	0.23	B0 Ib	
95	HD 167659	12.20	-1.27	7.60	7.39	0.53	O7 II-IIIIf	(7.36,1.80)
96	HD 167771	12.70	-1.13	6.66	6.54	0.44	O7 IIIIf	(6.53,1.49)
97	HD 167971	18.25	+1.68	8.27	7.50	1.08	O8 Iafn	(7.45,3.66)
98	HD 168076	16.84	+0.84	8.61	8.18	0.75	O4 IIIIf	(8.20,2.94)
99	HD 168941	5.82	-6.31	9.41	9.34	0.37	O9.5 IVp	(9.36,1.18)
100	HD 172140	5.28	-10.61	9.90	9.96	0.22	B0.5 III	
101	HD 175754	16.39	-9.92	6.93	7.01	0.23	O8 IIIfp	(7.01,0.85)
102	HD 175876	15.28	-10.58	6.81	6.92	0.21	O6.5 IIIIf	(6.93,0.68)
103	HD 177989	17.81	-11.88	9.28	9.33	0.25	B0 III	
104	HD 178487	25.78	-8.56	8.82	8.66	0.40	B0 Ib	

Table 1 *continued*

Table 1 (*continued*)

ID	Target	ℓ	b	B	V	$E(B - V)$	SpT	GOS
		(deg)	(deg)	(mag)	(mag)	(mag)		(V_J, A_{V_J})
105	HD 179406	28.23	-8.31	5.47	5.34	0.33	B3 IV	
106	HD 179407	24.02	-10.40	9.50	9.41	0.33	B0.5 Ib	
107	HD 185418	53.60	-2.17	7.67	7.45	0.50	B0.5 V	
108	HD 187459	68.81	+3.85	6.64	6.49	0.44	B0.5 Ib	
109	HD 190429A	72.59	+2.61	7.20	7.09	0.43	O4 If	(6.57,1.50)
110	HD 190918	72.65	+2.07	6.88	6.75	0.45	O9.5 Iab+WN4	
111	HD 191495	72.74	+1.41	8.51	8.41	0.40	B0 IV-V	
112	HD 191877	61.57	-6.45	6.27	6.28	0.21	B1 Ib	
113	HD 192035	83.33	+7.76	8.23	8.18	0.35	B0 III-IVn	
114	HD 192639	74.90	+1.48	7.46	7.11	0.66	O7.5 Iab	(7.11,2.03)
115	HD 195965	85.71	+5.00	6.93	6.98	0.25	B0 V	
116	HD 199579	85.70	-0.30	6.01	5.96	0.37	O6.5 Vfz	(5.95,1.17)
117	HD 201345	78.44	-9.54	7.61	7.76	0.15	ON9.2 IV	(7.74,0.51)
118	HD 201638	80.29	-8.45	8.92	9.05	0.11	B0.5 Ib	
119	HD 203374A	100.51	+8.62	6.91	6.67	0.53	B0 IVpe	
120	HD 206267	99.29	+3.74	5.82	5.62	0.53	O6 Vf	(5.67,1.58)
121	HD 206773	99.80	+3.62	7.12	6.91	0.51	B0 Vpe	
122	HD 207198	103.1	+6.99	6.27	5.96	0.60	O8.5 II	(5.92,1.69)
123	HD 207308	103.11	+6.82	7.74	7.49	0.53	B0.5 V	
124	HD 208440	104.03	+6.44	7.93	7.91	0.28	B1 V	
125	HD 209339	104.58	+5.87	6.73	6.73	0.30	O9.7 IV	(6.70,1.10)
126	HD 210809	99.85	-3.13	7.59	7.54	0.34	O9 Iab	(7.55,1.15)
127	HD 210839	103.83	+2.61	5.30	5.05	0.57	O6.5 Infp	(5.05,1.61)
128	HD 216044	105.93	-3.64	8.59	8.51	0.38	B0 III-IV	
129	HD 216532	109.65	+2.68	8.54	8.00	0.85	O8.5 Vn	(8.00,2.58)
130	HD 216898	109.93	+2.39	8.53	8.00	0.84	O9 V	(8.01,2.52)
131	HD 217035	110.25	+2.86	8.20	7.74	0.74	B0.5 V	
132	HD 217312	110.56	+2.95	7.81	7.42	0.67	B0.5 V	
133	HD 218915	108.06	-6.89	7.22	7.20	0.30	O9.2 Iab	(7.20,0.95)
134	HD 224151	115.44	-4.64	6.01	6.19	0.44	B0.5 II-III	
135	HD 224257	115.25	-6.06	7.92	7.98	0.24	B0.2 IV	
136	HD 224868	116.87	-1.44	7.39	7.29	0.34	B0 Ib	
137	HD 303308	287.59	-0.61	8.33	8.19	0.46	O4.5 Vfc	(8.12,1.57)
138	HD 308813	294.79	-1.61	9.32	9.28	0.34	O9.7 IVn	(9.28,1.16)
139	HD 332407	64.28	+3.11	8.63	8.50	0.41	B0.5 III	

^a Updated photometry and extinction (V_J, A_{V_J}) from the GOS survey (Maiz Apéllániz & Barbá 2018). In multiple systems, the quoted magnitude is that of the brightest stellar component. We analyze HD 93129A and HD 93206A as binary systems (Aa, Ab) – see Gruner et al. (2019), Parkin et al. (2011), and further discussion in Appendix A.

Table 2. Stellar Distance Estimates^a (D_i in kpc)

ID	Star Name	SpT	Refs	D_{Gaia}	D_{Bowen}	D_{Savage}	D_{Shull}	D_{GOS}
				(DR2-2018)	(2008)	(2001)	(2019)	(2019)
1	BD 35°4258	B0.5 Vn	8,25	1.89[1.71,2.10]			2.51	
2	BD 53°2820	B0 IVn	14,25	3.18[2.82,3.65]	4.8[3.6,6.4]		4.27	
3	CPD-59°2600	O6 Vf	2,14	5.11[4.28,6.36]	2.9[2.6,3.6]	2.84	2.71	2.11
4	CPD-59°2603	O7 Vnz	2,14	3.66[3.22,4.22]	3.5[3.1,4.4]	2.68	2.81	2.60
5	CPD-69°1743	B0.5 IIIn	10,11	3.43[3.04,3.93]		4.68	4.47	
6	CPD-72°1184	B0 III	16	6.88[5.46,9.32]		9.41	9.85	
7	HD 3827	B0.7 V	26	2.15[1.85,2.59]		2.04	1.88	

Table 2 *continued*

Table 2 (continued)

ID	Star Name	SpT	Refs	D_{Gaia}	D_{Bowen}	D_{Savage}	D_{Shull}	D_{GOS}
				(DR2-2018)	(2008)	(2001)	(2019)	(2019)
8	HD 5005A	O4 Vfc	1,8	2.71[2.39,3.14]	2.9[2.8,3.1]	2.28	3.13	2.89
9	HD 12323	ON9.2 V	2,28	2.59[2.33,2.93]	4.4[3.9,5.8]	2.89	2.81	3.04
10	HD 13268	ON8.5 IIIIn	1,28	1.61[1.50,1.74]	2.1[1.8,2.7]	1.75	2.77	2.80
11	HD 13745	O9.7 IIIn	1,9	2.13[1.91,2.39]	3.2[2.2,3.9]	2.91	2.80	2.81
12	HD 14434	O5.5 Vnfp	1,28	2.37[2.13,2.67]	3.5[3.1,4.3]	3.17	2.95	2.98
13	HD 15137	O9.5 II-IIIIn	1,26	3.33[2.86,4.00]	3.5[2.2,4.9]	3.01	2.88	3.00
14	HD 15558A	O4.5 IIIf	2,26	2.02[1.72,2.44]			2.01	1.91
15	HD 15642	O9.5 II-IIIIn	1,26	3.69[3.20,4.34]		3.41	3.75	3.89
16	HD 34656	O7.5 IIIf	1,28	2.32[1.92,2.93]	2.2[1.9,2.7]	2.12	2.10	1.99
17	HD 39680	O6 Vnfp	1,28	3.07[2.57,3.79]	2.6[2.3,3.2]	2.80	2.67	
18	HD 41161	O8 Vn	1,17	1.52[1.40,1.66]	1.4[1.2,1.8]	1.23	1.35	1.16
19	HD 42088	O6 Vfz	1,9	1.65[1.50,1.83]	2.0[1.7,2.5]	2.15	2.03	1.97
20	HD 45314	O9npe	9	0.80[0.78,0.84]	2.1[0.8,3.6]	0.80	0.80	
21	HD 46150	O5 Vf	1,9	1.52[1.36,1.73]	1.7[1.5,2.0]	1.48	1.49	1.47
22	HD 47360	B0.5 V	9	1.32[1.17,1.51]	1.5[1.3,2.0]	1.27	1.24	
23	HD 47417	B0 IV	9	1.49[1.35,1.66]	1.3[1.0,1.8]	1.15	1.23	
24	HD 60369	O9 IV	10,11	3.10[2.97,4.03]	2.7[2.1,3.6]		2.54	
25	HD 61347	O9 Ib	9,28	8.16[6.11,12.3]	4.4[3.6,5.4]	4.44	4.44	
26	HD 62866	B0.5 IIIn	10,11	3.81[[3.28,4.54]	3.9[2.9,5.5]		3.51	
27	HD 63005	O7 Vf	3,10,11	9.70 [6.38,20.1]	5.4[4.7,6.6]	5.23	4.35	
28	HD 64568	O3 Vf* z	2,10,11	6.00[4.87,7.80]	6.5[5.7,7.7]		6.41	5.75
29	HD 66695	B0.5 IV	10,11	3.21[2.72,3.92]			4.25	
30	HD 66788	O8 V	10,11,49	4.90[3.85,6.74]	4.3[3.7,5.6]	4.30	4.72	
31	HD 69106	B0.2 V	2,3	1.24[1.17,1.33]	1.5[1.1,2.0]	1.49	1.12	1.10
32	HD 73882	O8.5 IV	2,10,11	0.34[0.30,0.41]		0.79	1.00	0.83
33	HD 74194	O8.5 Ib-II	2,10,11	2.20[2.07,2.36]		2.80	2.58	2.25
34	HD 74920	O7.5 IVn	2,4,46	2.65[2.42,2.92]	3.6[1.6,6.1]	1.50	2.09	2.05
35	HD 89137	ON9.7 IIIn	2,10,11	3.46[3.05,4.00]	3.1[2.3,4.4]	2.97	4.16	4.04
36	HD 90087	O9.2 III	2,10,11	2.93[2.62,3.32]	2.8[2.2,3.7]	2.74	2.69	2.52
37	HD 91597	B1 III ne	10,11	6.89[5.61,8.90]	3.9[3.1,6.0]	4.19	4.29	
38	HD 91651	ON9.5 IIIIn	2,10,11	1.83[1.69,2.00]	2.8[2.5,3.7]	2.81	4.31	3.98
39	HD 91824	O7 Vfz	2,10,11	2.18[1.99,2.41]			2.84	2.75
40	HD 92554	O9.5 IIIn	10,11	4.04[3.53,4.72]	6.9[5.0,8.4]	6.80	6.61	
41	HD 93028	O9 IV	2,12	3.18[2.72,3.83]			2.95	2.97
42	HD 93129A	O2 If*	2,42	2.83[2.60,3.11]	2.8[2.2,3.4]		2.49	2.21
43	HD 93146A	O7 Vfz	2,21,24	3.14[2.80,3.58]	3.5[3.1,4.3]	3.41	2.84	2.30
44	HD 93204	O5.5 V	2,31	2.09[1.94,2.27]		3.48	3.25	2.73
45	HD 93205	O3.5 V	2,31	2.49[2.27,2.76]	3.3 [3.0,3.9]	2.54	2.82	2.44
46	HD 93206A	O9.7 IIn	2,21	1.07[0.96,1.20]	2.6[2.2,3.2]	1.78	2.23	1.48
47	HD 93222AB	O7 IIIIf	2,3	2.70[2.47,2.99]	3.6[2.8,4.2]	3.26	3.39	2.47
48	HD 93250	O4 IIIIfc	2,24,31	2.54[2.36,2.75]	2.3[2.1,2.7]	1.89	2.62	2.20
49	HD 93843	O5 IIIIf	2,10,11	2.43[2.24,2.66]	3.5[2.8,4.0]	3.68	3.21	2.85
50	HD 96670	O8 Ibf	10,11,32	3.59[3.19,4.09]	3.8[3.1,4.6]	2.88	2.78	2.67
51	HD 96715	O4 Vf	2,10,11	3.25[2.94,3.63]	3.8[3.4,4.6]	3.12	3.52	3.15
52	HD 96917	O8 Ib	2,10,11	4.41[3.72,5.43]	2.9[2.4,3.6]	2.68	2.61	2.46
53	HD 97471	B0 V	12,13	4.86[3.85,6.58]			2.78	
54	HD 97913	B0.5 IVn	10,11	3.40[2.97,3.97]	2.6[1.9,3.5]		2.52	
55	HD 99857	B0.5 Ib	10,11	2.17[2.04,2.33]	3.5[2.7,4.5]	3.06	3.04	
56	HD 99890	B0 IIIn	10,11	1.85[1.70,2.03]	3.5[2.6,5.2]	3.07	3.22	
57	HD 100199	B0 IIIn	10,11	1.25[1.15,1.37]	3.3[2.5,5.0]		2.77	
58	HD 100213	O8 Vn	2,10,11	2.21[2.03,2.42]	2.6[2.3,3.3]	2.06	2.26	2.15
59	HD 100276	B0.5 Ib	10,11	2.62[2.40,2.89]	3.2[2.4,4.1]	2.96	2.94	
60	HD 101131	O5.5 Vf	2,21	2.44[2.07,2.97]	2.0[1.7,2.4]	1.91	2.08	1.78

Table 2 continued

Table 2 (continued)

ID	Star Name	SpT	Refs	D_{Gaia}	D_{Bowen}	D_{Savage}	D_{Shull}	D_{GOS}
				(DR2-2018)	(2008)	(2001)	(2019)	(2019)
61	HD 101190	O6 IVf	2,10,11	3.06[2.73,3.47]	2.1[1.8,2.6]	1.95	2.16	2.09
62	HD 101205	O7 II:	2,10,11	2.63[1.94,4.08]	2.4[1.9,2.8]	1.47	1.68	1.64
63	HD 101298	O6.5 IVf	2,10,11	2.50[2.31,2.74]	2.8[2.4,3.4]	2.72	2.85	2.58
64	HD 101413	O8 V	2,10,11	1.78[1.65,1.94]	2.4[2.1,3.1]	2.12	2.33	2.13
65	HD 101436	O6.5 Vf	2,10,11	2.81[2.18,3.95]	2.2[1.9,2.7]	2.17	1.93	1.85
66	HD 103779	B0.5 Iab	10,11	2.22[2.06,2.41]	4.3[3.4,5.6]	4.07	3.99	
67	HD 104705	B0 Ib	10,11	2.16[1.99,2.36]	5.0[4.1,6.1]	3.90	4.18	
68	HD 115071	O9.5 III	2,10,11	1.98[1.84,2.14]	1.2[1.0,1.7]	1.01	2.05	1.87
69	HD 116781	B0 IIIne	10,11	1.93[1.77,2.12]	2.2[1.7,3.3]	1.71	1.79	
70	HD 116852	O8.5 II-III f	2,16	13 [7.7,18]		4.76	4.83	4.88
71	HD 118571	B0.5 IVn	10,11	2.32[2.09,2.60]	2.9[2.1,4.0]		2.70	
72	HD 124314A	O6 IVnf	2,6	1.72[1.62,1.83]	1.4[1.2,1.7]	1.15	1.27	1.25
73	HD 124979	O7.5 IVn	2,16	3.10[2.71,3.63]	2.8[2.5,3.6]	2.18	3.05	3.09
74	HD 148422	B1 Ia	10,11	5.74[4.53,7.84]	10[7.4,11]	8.84	8.26	
75	HD 152218	O9 IVn	2,33	1.89[1.73,2.08]	1.9[1.4,2.5]	1.48	1.53	1.42
76	HD 152233	O6 III f	2,21	1.70[1.57,1.86]	2.3[1.8,2.6]	1.44	1.66	1.52
77	HD 152248	O7 Iabf	2,33	1.62[1.48,1.78]	2.2[1.8,2.7]	1.57	1.76	1.61
78	HD 152314	O9 IV	2,33	1.54[1.42,1.67]	2.7[1.7,4.1]	1.93	1.67	1.44
79	HD 152623	O7 Vnf	2,33	neg parallax	1.5[1.3,1.9]	1.11	1.16	1.04
80	HD 152723	O6.5 III	2,10,11	large errors	2.3[1.9,2.6]	1.82	2.00	1.94
81	HD 153426	O8.5 III	2,34	2.03[1.84,2.27]	2.6[1.7,3.5]	2.32	1.97	1.83
82	HD 154368	O9.2 Iab	2,10,11	1.17[1.11,1.25]		1.35	1.08	1.08
83	HD 156292	O9.7 III	2,10,11	1.74[1.55,1.98]	1.7[1.3,2.4]	1.62	1.48	1.51
84	HD 157857	O6.5 II	1,16	3.55[2.89,4.61]	3.1[2.5,3.5]	2.36	2.71	2.56
85	HD 158661	B0.5 Ib	8	2.55[2.23,2.99]	4.2[3.2,5.4]		4.08	
86	HD 161807	O9.7 III n	2,10,11	1.27[1.18,1.37]	2.1[1.5,3.1]		1.86	1.94
87	HD 163758	O6.5 Ia fp	2,10,11	3.47[2.82,4.50]	4.7[3.9,5.3]	4.47	4.34	4.11
88	HD 163892	O9.5 IVn	2,10,11	1.39[1.28,1.52]	1.6[1.2,2.1]	1.57	1.38	1.37
89	HD 164816	O9.5 V	2,10,11	1.14[1.06,1.24]		1.69	1.13	1.08
90	HD 165052	O5.5: Vz	2,10,11	1.23[1.16,1.30]	1.9[1.6,2.3]	1.48	1.52	1.37
91	HD 165246	O8 Vn	2,10,11	1.88[1.55,2.39]			1.64	1.38
92	HD 166546	O9.5 IV	2,21,28	1.56[1.35,1.84]			1.48	1.46
93	HD 166716	B0 II-III	8	1.69[1.50,1.92]			2.73	
94	HD 167402	B0 Ib	10,11	< 14 kpc	9.0[5.7,12.2]	7.04	7.61	
95	HD 167659	O7 II-III f	1,10,11	1.58[1.40,1.80]	2.5[2.1,3.0]	2.14	2.04	1.87
96	HD 167771	O7 III f	2,28	1.82[1.67,2.00]	2.3[1.8,2.6]	1.43	1.50	1.40
97	HD 167971	O8 Ia f	1,9	1.92[1.58,2.43]			1.68	1.42
98	HD 168076	O4 III f	1,35	neg parallax			2.58	1.97
99	HD 168941	O9.5 IV p	2,10,11	2.32[1.96,2.84]	6.8[4.4,9.6]	5.79	3.75	3.72
100	HD 172140	B0.5 III	15,36	< 9.6 kpc		6.47	6.54	
101	HD 175754	O8 II nfp	2,10,11	2.07[1.85,2.35]	2.8[2.3,3.5]	2.75	2.71	2.55
102	HD 175876	O6.5 III n f	2,16,28	2.54[2.15,3.10]		2.36	2.59	2.57
103	HD 177989	B0 III	16	2.48[2.17,2.87]		4.91	5.14	
104	HD 178487	B0 Ib	16	3.35[2.87,4.04]	5.7[4.3,7.2]	4.83	5.22	
105	HD 179406	B3 IV	47,48	0.28[0.27,0.30]			0.21	
106	HD 179407	B0.5 Ib	16,18	3.09[2.69,3.63]		7.76	7.72	
107	HD 185418	B0.5 V	8,9	0.74[0.72,0.76]	1.2[1.1,1.7]		0.78	
108	HD 187459	B0.5 Ib	8,9	1.39[1.31,1.48]	2.2[1.6,2.7]	1.69	1.68	
109	HD 190429A	O4 If	1,6,37	2.04[1.91,2.20]	2.9[2.1,3.8]	1.80	2.57	2.38
110	HD 190918	O9.7 Iab+WN4	5,21	1.85[1.74,1.97]	2.1[1.7,2.6]	2.59	2.39	
111	HD 191495	B0 IV-V	8,18,38	1.60[1.48,1.74]	1.8[1.6,2.4]		1.69	
112	HD 191877	B1 Ib	8,39	1.34[1.23,1.48]	2.3[1.5,3.0]	2.21	2.07	
113	HD 192035	B0 III-IV	18,40	2.11[1.94,2.31]	2.7[1.7,4.6]	2.19	2.31	

Table 2 continued

Table 2 (*continued*)

ID	Star Name	SpT	Refs	D_{Gaia}	D_{Bowen}	D_{Savage}	D_{Shull}	D_{GOS}
				(DR2-2018)	(2008)	(2001)	(2019)	(2019)
114	HD 192639	O7.5 Iabf	1,9,37	2.41[2.23,2.62]	2.1[1.7,2.6]		2.13	2.14
115	HD 195965	B0 V	9	0.84[0.81,0.87]	1.1[1.0,1.5]	0.91	1.03	
116	HD 199579	O6.5 V	1,9	0.91[0.87,0.97]	1.4[1.3,1.7]	1.05	0.94	0.92
117	HD 201345	ON9.2 IV	2,20	2.91[2.51,3.46]	2.2[1.9,2.9]	1.91	2.56	2.50
118	HD 201638	B0.5 Ib	19,45	3.32[2.81,4.06]			8.95	
119	HD 203374	B0 IVpe	20,30	large error			0.78	
120	HD 206267	O6 Vf	7,27,30	1.08[0.86,1.45]		0.72	0.69	0.73
121	HD 206773	B0 Vpe	9,30	0.93[0.91,0.96]			0.69	
122	HD 207198	O8.5 IIf	2,28	0.99[0.94,1.05]	1.3[0.9,1.7]		0.98	1.04
123	HD 207308	B0.5 V	30,40	0.99[0.96,1.03]			0.76	
124	HD 208440	B1 V	22,30	0.81[0.79,0.83]			1.04	
125	HD 209339	O9.7 IV	2,20	0.82[0.80,0.85]			1.18	1.08
126	HD 210809	O9 Iab	1,9	3.83[3.37,4.42]	4.3[3.5,5.5]	4.01	4.05	3.88
127	HD 210839	O6.5 Infp	1,9,30	0.61[0.56,0.66]	1.1[0.8,1.5]	0.81	0.81	0.87
128	HD 216044	B0 III-IV	9,18	2.84[2.53,3.25]	5.4[3.6,6.6]		2.57	
129	HD 216532	O8.5 Vn	1,23	0.73[0.72,0.75]			0.92	0.94
130	HD 216898	O9 V	1,9,23	0.82[0.80,0.84]			0.87	0.91
131	HD 217035	B0.5 V	9,23	0.81[0.79,0.83]			0.72	
132	HD 217312	B0 V	23,39	1.56[1.15,2.36]			0.60	
133	HD 218915	O9.2 Iab	2,9	6.5 [5.0,9.4]	5.0[4.1,6.4]	3.63	3.66	3.62
134	HD 224151	B0.5 II-III	9,29	1.80[1.63,2.01]	1.4[1.0,1.9]	1.01	0.91	
135	HD 224257	B0.2 IV	9,18	1.90[1.75,2.08]			2.05	
136	HD 224868	B0 Ib	20	0.78[0.73,0.83]	3.1[2.5,3.8]		3.03	
137	HD 303308	O4.5 Vfc	2,14,31	2.29[2.10,2.51]	3.8[3.4,4.5]	2.85	2.93	2.66
138	HD 308813	O9.7 IVn	2,32,41	4.56[3.87,5.53]	3.1[2.7,4.1]	2.92	3.61	3.45
139	HD 332407	B0.5 III	6,18,44	2.64[2.39,2.95]	2.6[1.9,2.7]	2.41	2.56	

^a Columns 3 and 4 give references to our choices of SpTs and (B, V) in Table 1 used to estimate E(B-V). Many SpTs are from the GOS survey (Maíz Apellániz et al. 2004; Sota et al. 2011, 2014). Column 5 gives the corrected Gaia parallax distance D_{Gaia} and quoted errors for 135 stars, after applying the 0.03 mas offset. Columns 6 and 7 give photometric distances from two previous surveys of interstellar matter: D_{Savage} (Savage et al. 2001) and D_{Bowen} (Bowen et al. 2008). Columns 8 and 9 provide two new photometric distances from this study: D_{Shull} calculated from original photometry sources (footnote b); and D_{GOS} using the subset of O-type stars from the GOS survey with updated spectral types (Sota et al. 2011, 2014) and digital photometry and extinction (Maíz Apellániz & Barbá 2018). Absolute magnitudes (M_V) are from Vacca et al. (1996) and Bowen et al. (2008) in Table 11 of their Appendix B3. Further discussion of discrepancies in stellar distances is provided in Appendix A of this paper, primarily arising from stellar properties (SpT, photometry, extinction, binaries). Our survey includes 84 O-type stars in the GOS survey (Sota et al. 2011, 2014) and other original sources for SpT and photometry labeled as follows: (1) Sota et al. 2011; (2) Sota et al. 2014; (3) Markova et al. 2011; (4) Thackeray & Andrews 1974; (5) Walborn et al. 2002; (6) Walborn 1973a; (7) Saurin et al. 2012; (8) Morgan et al. 1955; (9) Hiltner 1956; (10) Garrison et al. 1977; (11) Schild et al. 1983; (12) Reed & Beatty 1995; (13) Zsargo et al. 2003; (14) Humphreys 1978; (15) Hill 1970; (16) Hill et al. 1974; (17) Hill & Lynas 1977; (18) Walborn 1971; (19) Bidelman 1951; (20) Hog et al. 2000; (21) Ducati 2002; (22) Blaauw et al. 1959; (23) Garrison 1970; (24) Maíz Apellániz et al. 2016; (25) Wesselius et al. 1982; (26) Deutschman et al. 1976; (27) Johnson & Morgan 1955; (28) Hiltner & Johnson 1956; (29) Lesh 1968; (30) Pan et al. 2004; (31) Massey & Johnson 1993; (32) Maíz Apellániz & Barba 2018; (33) Schild et al. 1969; (34) Crampton 1971; (35) Hillenbrand et al. 1995; (36) Tripp et al. 1993; (37) Bouret et al. 2012; (38) Mermilliod & Mermilliod 1994; (39) Fernie 1983; (40) Guetter 1974; (41) Schild 1970; (42) Gruner et al. 2019; (43) Levato & Malaroda 1981; (44) Howarth et al. 1997; (45) Simbad database; (46) Vijapurkar & Drilling 1993; (47) Buscombe 1962; (48) Braganca et al. 2012; (49) MacConnell & Bidelman (1976).

Table 3. Parallax Errors and Distance Estimates^a (D_i in kpc)

ID	Star Name	SpT	Parallax	Ratio	G_{Gaia}	D_{Gaia}	D_{Shull}	D_{GOS}	Ratio
			$\varpi \pm \sigma_\varpi$ (mas)	ϖ/σ_ϖ	(mag)	(DR2-2018)	(2019)	(2019)	Gaia/GOS
3	CPD-59°2600	O6 Vf	0.1655 ± 0.0382	4.3	8.46	5.11[4.28-6.36]	2.71	2.11	2.42
4	CPD-59°2603	O7 Vnz	0.2435 ± 0.0368	6.6	8.69	3.66[3.22-4.22]	2.81	2.60	1.41
8	HD 5005A	O4 Vfc	0.3388 ± 0.0500	6.8	8.52	2.71[2.39-3.14]	3.13	2.89	0.94

Table 3 *continued*

Table 3 (continued)

ID	Star Name	SpT	Parallax	Ratio	G_{Gaia}	D_{Gaia}	D_{Shull}	D_{GOS}	Ratio
			$\varpi \pm \sigma_{\varpi}$ (mas)	ϖ/σ_{ϖ}	(mag)	(DR2-2018)	(2019)	(2019)	Gaia/GOS
9	HD 12323	ON9.2 V	0.3557 ± 0.0442	8.1	8.90	2.59[2.33-2.93]	2.81	3.04	0.85
10	HD 13268	ON8.5 IIIIn	0.5906 ± 0.0466	12.7	8.11	1.61[1.50-1.74]	2.77	2.80	0.58
11	HD 13745	O9.7 IIIn	0.4405 ± 0.0528	8.3	7.78	2.13[1.91-2.39]	2.80	2.81	0.76
12	HD 14434	O5.5 Vnfp	0.3912 ± 0.0473	8.3	8.43	2.37[2.13-2.67]	2.95	2.98	0.85
13	HD 15137	O9.5 II-IIIIn	0.2700 ± 0.0502	5.4	7.81	3.33[2.86-4.00]	2.88	3.00	1.11
14	HD 15558A	O4.5 IIIIf	0.4655 ± 0.0855	5.4	7.77	2.02[1.72-2.44]	2.01	1.91	1.06
15	HD 15642	O9.5 II-IIIIn	0.2412 ± 0.0410	5.9	8.49	3.69[3.20-4.34]	3.75	3.89	0.95
16	HD 34656	O7.5 IIIf	0.4012 ± 0.0896	4.5	6.72	2.32[1.92-2.93]	2.10	1.99	1.17
18	HD 41161	O8 Vn	0.6284 ± 0.0575	10.9	6.71	1.52[1.40-1.66]	1.35	1.16	1.31
19	HD 42088	O6 Vfz	0.5752 ± 0.0593	9.7	7.48	1.65[1.50-1.83]	2.03	1.97	0.84
21	HD 46150	O5 Vf	0.6263 ± 0.0788	7.9	6.70	1.52[1.36-1.73]	1.49	1.47	1.03
28	HD 64568	O3 Vf* z	0.1367 ± 0.0386	3.5	9.31	6.00[4.87-7.80]	6.41	5.75	1.04
31	HD 69106	B0.2 V	0.7743 ± 0.0507	15.3	7.08	1.24[1.17-1.33]	1.12	1.10	1.13
32	HD 73882	O8.5 IV	2.8856 ± 0.4507	6.4	7.22	0.34[0.30-0.41]	1.00	0.83	0.41
33	HD 74194	O8.5 Ib-II	0.4236 ± 0.0300	14.1	7.44	2.20[2.07-2.36]	2.58	2.25	0.98
34	HD 74920	O7.5 IVn	0.3479 ± 0.0358	9.7	7.48	2.65[2.42-2.92]	2.09	2.05	1.29
35	HD 89137	ON9.7 IIIn	0.2588 ± 0.0390	6.6	7.94	3.46[3.05-4.00]	4.16	4.04	0.86
36	HD 90087	O9.2 III	0.3117 ± 0.0409	7.6	7.72	2.93[2.62-3.32]	2.69	2.52	1.16
38	HD 91651	ON9.5 IIIIn	0.5167 ± 0.0445	11.6	8.81	1.83[1.69-2.00]	4.31	3.98	0.46
39	HD 91824	O7 Vfz	0.4291 ± 0.0441	9.7	8.11	2.18[1.99-2.41]	2.84	2.75	0.79
41	HD 93028	O9 IV	0.2844 ± 0.0534	5.3	8.34	3.18[2.72-3.83]	2.95	2.97	1.07
42	HD 93129A	O2 If*	0.3233 ± 0.0316	10.2	7.17	2.83[2.60-3.11]	2.49	2.21	1.28
43	HD 93146A	O7 Vfz	0.2880 ± 0.0386	7.5	8.35	3.14[2.80-3.58]	2.84	2.30	1.37
44	HD 93204	O5.5 V	0.4486 ± 0.0378	11.9	8.36	2.09[1.94-2.27]	3.25	2.73	0.77
45	HD 93205	O3.5 V	0.3719 ± 0.0391	9.5	8.65	2.49[2.27-2.76]	2.82	2.44	1.02
46	HD 93206A	O9.7 Ibn	0.9084 ± 0.1018	8.9	6.24	1.07[0.96-1.20]	2.23	1.48	0.72
47	HD 93222AB	O7 IIIIf	0.3399 ± 0.0356	9.5	8.01	2.70[2.47-2.99]	3.39	2.47	1.09
48	HD 93250	O4 IIIIfc	0.3631 ± 0.0300	12.1	7.26	2.54[2.36-2.75]	2.62	2.20	1.15
49	HD 93843	O5 IIIIf	0.3808 ± 0.0347	11.0	7.26	2.43[2.24-2.66]	3.21	2.85	0.85
50	HD 96670	O8 Ibf	0.2488 ± 0.0344	7.2	7.34	3.59[3.19-4.09]	2.78	2.67	1.34
51	HD 96715	O4 Vf	0.2777 ± 0.0321	8.7	8.18	3.25[2.94-3.63]	3.52	3.15	1.03
52	HD 96917	O8 Ib	0.1966 ± 0.0423	4.6	7.00	4.41[3.72-5.43]	2.61	2.46	1.79
58	HD 100213	O8 Vn	0.4224 ± 0.0391	10.8	8.53	2.21[2.03-2.42]	2.26	2.85	0.78
60	HD 101131	O5.5 Vf	0.3795 ± 0.0729	5.2	7.07	2.44[2.07-2.97]	2.08	1.78	1.37
61	HD 101190	O6 IVf	0.2971 ± 0.0389	7.6	7.26	3.06[2.73-3.47]	2.16	2.09	1.46
62	HD 101205	O7 II:	0.3557 ± 0.1354	2.6	9.71	2.63[1.94-4.08]	1.68	1.64	1.60
63	HD 101298	O6.5 IVf	0.3693 ± 0.0340	10.9	8.00	2.50[2.31-2.74]	2.85	2.58	0.97
64	HD 101413	O8 V	0.5305 ± 0.0440	12.1	8.30	1.78[1.65-1.94]	2.33	2.13	0.84
65	HD 101436	O6.5 Vf	0.3207 ± 0.1027	3.2	7.52	2.81[2.18-3.95]	1.93	1.85	1.52
68	HD 115071	O9.5 III	0.4758 ± 0.0379	12.6	7.85	1.98[1.84-2.14]	2.05	1.87	1.06
70	HD 116852	O8.5 II-IIIIf	0.0440 ± 0.0564	0.78	8.43	13 [7.7-18]	4.83	4.88	2.66
72	HD 124314A	O6 IVnf	0.5530 ± 0.0360	15.4	6.74	1.72[1.62-1.83]	1.27	1.25	1.38
73	HD 124979	O7.5 IVn	0.2927 ± 0.0468	6.3	8.49	3.10[2.71-3.63]	3.05	3.09	1.00
75	HD 152218	O9 IVn	0.4990 ± 0.0491	10.2	7.51	1.89[1.73-2.08]	1.53	1.42	1.33
76	HD 152233	O6 IIf	0.5573 ± 0.0489	11.4	6.50	1.70[1.57-1.86]	1.66	1.52	1.12
77	HD 152248	O7 Iabf	0.5886 ± 0.0583	10.1	5.97	1.62[1.48-1.78]	1.76	1.61	1.01
78	HD 152314	O9 IV	0.6199 ± 0.0518	12.0	7.79	1.54[1.42-1.67]	1.67	1.44	1.07
81	HD 153426	O8.5 III	0.4623 ± 0.0511	9.0	7.38	2.03[1.84-2.27]	1.97	1.83	1.11
82	HD 154368	O9.2 Iab	0.8218 ± 0.0490	16.8	5.92	1.17[1.11-1.25]	1.08	1.08	1.08
83	HD 156292	O9.7 III	0.5455 ± 0.0699	7.8	7.42	1.74[1.55-1.98]	1.48	1.51	1.15
84	HD 157857	O6.5 II	0.2517 ± 0.0648	3.9	7.70	3.55[2.89-4.61]	2.71	2.56	1.39
86	HD 161807	O9.7 IIIIn	0.7576 ± 0.0602	12.6	6.97	1.27[1.18-1.37]	1.86	1.94	0.65
87	HD 163758	O6.5 Iafp	0.2582 ± 0.0661	3.9	7.26	3.47[2.82-4.50]	4.34	4.11	0.84

Table 3 continued

Table 3 (continued)

ID	Star Name	SpT	Parallax	Ratio	G_{Gaia}	D_{Gaia}	D_{Shull}	D_{GOS}	Ratio
			$\varpi \pm \sigma_{\varpi}$ (mas)	ϖ/σ_{ϖ}	(mag)	(DR2-2018)	(2019)	(2019)	Gaia/GOS
88	HD 163892	O9.5 IVn	0.6901 ± 0.0635	10.9	7.38	1.39[1.28-1.52]	1.38	1.37	1.01
89	HD 164816	O9.5 V	0.8442 ± 0.0704	12.0	7.03	1.14[1.06-1.24]	1.13	1.08	1.06
90	HD 165052	O5.5: Vz	0.7837 ± 0.0460	17.0	6.77	1.23[1.16-1.30]	1.52	1.37	0.90
91	HD 165246	O8 Vn	0.5011 ± 0.1131	4.4	7.66	1.88[1.55-2.39]	1.64	1.38	1.36
92	HD 166546	O9.5 IV	0.6127 ± 0.0994	6.2	7.17	1.56[1.35-1.84]	1.48	1.46	1.07
95	HD 167659	O7 II-III f	0.6036 ± 0.0792	7.6	7.24	1.58[1.40-1.80]	2.04	1.87	0.84
96	HD 167771	O7 III f	0.5202 ± 0.0498	10.4	6.43	1.82[1.67-2.00]	1.50	1.40	1.30
97	HD 167971	O8 Iaf	0.4918 ± 0.1106	4.4	7.13	1.92[1.58-2.43]	1.68	1.42	1.35
99	HD 168941	O9.5 IVp	0.4018 ± 0.0792	5.1	9.28	2.32[1.96-2.84]	3.75	3.72	0.62
101	HD 175754	O8 II nfp	0.4529 ± 0.0566	8.0	6.95	2.07[1.85-2.35]	2.71	2.55	0.81
102	HD 175876	O6.5 III n f	0.3639 ± 0.0714	5.1	6.87	2.54[2.15-3.10]	2.59	2.57	0.99
109	HD 190429A	O4 I f	0.4599 ± 0.0349	13.2	6.98	2.04[1.91-2.20]	2.57	2.38	0.86
114	HD 192639	O7.5 Iab f	0.3850 ± 0.0336	11.5	7.00	2.41[2.23-2.62]	2.13	2.14	1.13
116	HD 199579	O6.5 V	1.0633 ± 0.0589	18.1	5.89	0.91[0.87-0.97]	0.94	0.92	0.99
117	HD 201345	ON9.2 IV	0.3135 ± 0.0548	5.7	7.72	2.91[2.51-3.46]	2.56	2.50	1.16
120	HD 206267	O6 Vf	0.8952 ± 0.2356	3.8	5.60	1.08[0.86-1.45]	0.69	0.73	1.48
122	HD 207198	O8.5 III f	0.9760 ± 0.0534	18.3	5.82	0.99[0.94-1.05]	0.98	1.04	0.95
125	HD 209339	O9.7 IV	1.1836 ± 0.0303	39.1	6.65	0.82[0.80-0.85]	1.18	1.08	0.76
126	HD 210809	O9 Iab	0.2313 ± 0.0351	6.6	5.50	3.83[3.37-4.42]	4.05	3.88	0.99
127	HD 210839	O6.5 Infp	1.6199 ± 0.1265	12.8	4.94	0.61[0.56-0.66]	0.81	0.87	0.70
129	HD 216532	O8.5 Vn	1.3316 ± 0.0299	44.5	7.81	0.73[0.72-0.75]	0.92	0.94	0.78
130	HD 216898	O9 V	1.1906 ± 0.0329	36.2	7.84	0.82[0.80-0.84]	0.87	0.91	0.90
133	HD 218915	O9.2 Iab	0.1241 ± 0.0472	2.6	7.17	6.49[4.97-9.35]	3.66	3.62	1.79
137	HD 303308	O4.5 Vfc	0.4071 ± 0.0393	10.4	8.06	2.29[2.10-2.51]	2.93	2.66	0.86
138	HD 308813	O9.7 IVn	0.1894 ± 0.0386	4.9	9.23	4.56[3.87-5.53]	3.61	3.45	1.32

^aOf the 84 stars with GOS classification and photometry, 81 have reliable *Gaia*-DR2 parallaxes, quantified by ϖ/σ_{ϖ} , the inverse of the relative parallax errors (columns 4 and 5). Column 6 lists *G* – band magnitudes from *Gaia*-DR2, which range from $G = 4.94$ (#127) to $G = 9.71$ (#62) with $\langle G \rangle = 7.51$. Columns 7, 8, 9 list distances (kpc) from *Gaia* and two photometric values, D_{Shull} and D_{GOS} , from Table 2. Column 10 lists the parallax-to-photometric distance ratio ($D_{\text{Gaia}}/D_{\text{GOS}}$), plotted in Figure 5 vs. a quality indicator (ϖ/σ_{ϖ}) of the parallax measurement.

Table 4. Carina OBI Distances^a

Star (ID)	SpT	$V_{J,0}$	A_{V_J}	$M_V^{(B)}$	$M_V^{(M)}$	D_{Gaia}	D_{phot}	D_{GOS}	D'_{GOS}	Cluster
		(mag)	(mag)	(mag)	(mag)	(kpc)	(kpc)	(kpc)	(kpc)	
HD 93204 (#44)	O5.5 V	6.827	1.611	-5.35	-5.07	2.09[1.94,2.27]	2.74	2.73	2.39	Tr 16
HD 93205 (#45)	O3.5 V	6.203	1.539	-5.73	-5.65	2.49[2.27,2.76]	2.38	2.43	2.34	Tr 16
HD 93250 (#48)	O4 III	5.515	1.850	-6.20	-5.98	2.54[2.36,2.75]	2.14	2.20	1.99	Tr 16
HD 303308 (#137)	O4.5 V	6.547	1.572	-5.57	-5.36	2.29[2.10,2.51]	2.43	2.66	2.40	Tr 16
CPD-59°2600 (#3)	O6 V	6.423	2.193	-5.20	-4.92	5.11[4.28,6.36]	2.18	2.11	1.86	Tr 16
CPD-59°2603 (#4)	O7 V	7.171	1.607	-4.90	-4.63	3.66[3.22,4.22]	2.32	2.60	2.29	Tr 16
CPD-59°2591	O8.5 V	7.682	3.123	-4.45	-4.19	2.32[2.10,2.58]	2.83	2.67	2.37	Tr 16
CPD-59°2626	O7.5 V	6.999	2.993	-4.75	-4.48	3.84[3.40,4.41]	2.40	2.24	1.98	Tr 16
CPD-59°2627	O9.5 V	8.195	1.920	-4.15	-3.90	2.67[2.46,2.91]	2.69	2.94	2.62	Tr 16
CPD-59°2628	O9.5 V	8.205	1.256	-4.15	-3.90	2.48[2.29,2.70]	2.48	2.96	2.64	Tr 16
CPD-59°2629	O8.5 V	7.452	3.378	-4.45	-4.19	2.15[2.02,2.30]	2.68	2.40	2.13	Tr 16
CPD-59°2634	O9.7 IV	7.603	2.137	-4.56	...	2.03[1.75,2.42]	2.49	2.71	...	Tr 16
CPD-59°2635	O8 V+O9.5 V	6.844	2.437	-4.60	-4.34	2.03[1.89,2.18]	2.73	2.50	2.23	Tr 16
CPD-59°2636	O8 V+O8 V	6.493	2.726	-4.60	-4.34	not available	2.48	2.34	2.03	Tr 16
CPD-59°2641	O6 V	6.636	2.579	-5.20	-4.92	2.13[1.99,2.30]	2.35	2.33	2.05	Tr 16
CPD-59°2644	O9 V	8.071	1.960	-4.30	-4.05	3.25[2.92,3.67]	3.03	2.98	2.66	Tr 16
HD 93129A (#42)	O2 I+O3 III	4.825	2.199	-6.49	-6.35	2.83[2.60,3.11]	1.97	2.21	1.72	Tr 14
HD 93128	O3.5 IV	6.532	2.243	-5.73	-5.65	3.14[2.88,3.45]	3.05	2.83	2.73	Tr 14
HD 93160	O7 III	5.897	1.952	-5.70	-5.54	3.56[3.12,4.14]	2.04	2.09	1.94	Tr 14
CPD-58°2620	O7 V	7.390	1.900	-4.90	-4.63	4.17[3.71,4.75]	2.72	2.87	2.54	Tr 14
CPD-58°2611	O6 V	7.237	2.356	-5.20	-4.92	2.92[2.71,3.17]	2.95	3.07	2.70	Tr 14
Tr 14-9	O8.5 V	7.450	2.454	-4.45	-4.19	2.17[2.01,2.36]	2.90	2.40	2.13	Tr 14
ALS 15204	O7.5 V	7.342	3.624	-4.75	-4.48	2.45[2.35,2.70]	2.90	2.62	2.31	Tr 14
ALS 15206	O9.2 V	7.882	2.785	-4.24	-3.99	2.83[2.63,3.07]	2.74	2.66	2.37	Tr 14
ALS 15207	O9 V	8.004	2.724	-4.30	-4.05	2.51[2.35,2.70]	3.12	2.89	2.58	Tr 14
HD 93028 (#41)	O9 IV	7.561	0.837	-4.80	...	3.18[2.72,3.83]	2.68	2.97	...	Coll 228
HD 93222 (#47)	O7 III	6.265	1.837	-5.70	-5.54	2.70[2.47,2.99]	2.91	2.47	2.30	Coll 228
HD 93146A (#43)	O7 V	6.905	1.535	-4.90	-4.63	3.14[2.80,3.58]	2.45	2.30	2.03	Coll 228
HD 93249A	O9 III	6.908	1.476	-5.30	-5.25	3.09[2.80,3.45]	2.52	2.76	2.70	Tr 15
Mean Distance						2.87	2.62	2.60	2.42	All stars
Standard Deviation						±0.73	±0.29	±0.28	±0.29	

^a Photometric distances and offset-corrected *Gaia* parallax distances for 29 stars associated with clusters (Trumpler 16, Trumpler 14, Trumpler 15, Collinder 228) in the Carina Nebula (Humphreys 1978; Alexander et al. 2016). We list D_{Gaia} (column 7) and three photometric distance estimates denoted: D_{phot} (column 8), D_{GOS} (column 9), and D'_{GOS} (column 10). D_{phot} is calculated using V and $E(B-V)$, as in Table 2, but with anomalous extinction, $R_V = A_V/E(B-V) = 4.0$ rather than $R_V = 3.1$. D_{GOS} is based on GOS digital photometry and extinction and the absolute magnitude grid (M_V) from Bowen et al. (2008). D'_{GOS} uses absolute magnitudes from Martins et al. (2005). Column 2 gives updated SpTs from the GOS spectroscopic survey (Sota et al. 2011, 2014). Columns 3 and 4 list the extinction-corrected visual magnitude ($V_{J,0} = V_J - A_{V_J}$) and visual extinction A_{V_J} from Maíz Apellániz & Barbá (2018). Column 5 lists absolute magnitudes (M_V) from Bowen et al. (2008) used for D_{phot} and D_{GOS} . Although the multiple system HD 93160 has previously been associated with Tr 16 (Walborn 1973b; Humphreys 1978), it more likely belongs in Tr 14 (see Fig. 12 of Sota et al. 2014). HD 93129A (ID #42) is a binary system (Gruner et al. 2019) whose GOS photometry is combined with HD 93129B; we exclude it from the statistics. For individual clusters, we find mean distances $\langle D_{\text{GOS}} \rangle$ for Tr 16 (2.55 ± 0.30 kpc), Tr 14 (2.68 ± 0.31 kpc), and Coll 228 (2.58 ± 0.23 kpc). Mean distances for the ensemble of all 29 O-stars are listed at the bottom of the table, with consistent photometric distances $\langle D_{\text{phot}} \rangle = 2.62 \pm 0.29$ kpc and $\langle D_{\text{GOS}} \rangle = 2.60 \pm 0.28$ kpc.

Table 5. Perseus OB1 Distances^a

Star (ID)	SpT	$V_{J,0}$	A_{V_J}	$M_V^{(B)}$	$M_V^{(M)}$	D_{Gaia}	D_{phot}	D_{GOS}	D'_{GOS}
		(mag)	(mag)	(mag)	(mag)	(kpc)	(kpc)	(kpc)	(kpc)
HD 12323 (#9)	ON9.2 V	8.176	0.736	-4.24	-3.99	2.59[2.33,2.93]	2.81	3.04	2.71
HD 13268 (#10)	ON8.5 III	6.836	1.340	-5.40	-5.32	1.61[1.50,1.74]	2.77	2.80	2.70
HD 13745 (#11)	O9.7 II	6.415	1.449	-5.83	...	2.13[1.91,2.39]	2.80	2.81	...
HD 14434 (#12)	O5.5 V	7.023	1.467	-5.35	-5.07	2.37[2.13,2.67]	2.95	2.98	2.62
HD 15137 (#13)	O9.5 II-III	6.865	1.007	-5.52	...	3.33[2.86,4.00]	2.88	3.00	...
HD 15642 (#15)	O9.5 II-III	7.432	1.098	-5.52	...	3.69[3.20,4.34]	3.75	3.89	...
HD 13022	O9.7 II-III	6.946	1.835	-5.47	...	2.26[2.04,2.52]	3.35	3.04	...
HD 12993	O6.5 V	7.512	1.454	-5.05	-4.77	2.41[2.17,2.70]	3.27	3.25	2.86
HD 14442	O5 III	6.974	2.242	-6.10	-5.84	3.50[3.12,3.97]	4.82	4.12	3.65
HD 16691	O4 If	6.152	2.523	-6.29	-6.34	2.13[1.95,2.35]	...	3.08	3.15
HD 14633	ON8.5 V	7.140	0.313	-4.45	-4.19	4.39[2.82,9.87]	2.10	2.08	1.85
HD 14947	O4.5 If	5.696	2.303	-6.64	-6.34	3.39[2.92,4.05]	2.76	2.93	2.55
Mean Distance						2.47	2.95	2.99	2.77
Standard Deviation						± 0.57	± 0.23	± 0.14	± 0.22

^a Same information as in Table 3 for 12 stars in Per OB1. As in Table 2, photometric distances D_{phot} were calculated from (B, V) photometry, SpTs (M_V), and extinction (A_V) assuming the standard value $R_V = A_V/E(B-V) = 3.1$. We present two GOS-based photometric distances, D_{GOS} and D'_{GOS} , with absolute magnitudes $M_V^{(B)}$ Bowen et al. (2008) and $M_V^{(M)}$ (Martins et al. 2005) respectively. In four cases (ellipses) SpTs are off the Martins et al. grid. Mean photometric distances based on the Bowen et al. (2008) grid are consistent with $\langle D_{\text{phot}} \rangle = 2.95 \pm 0.23$ kpc and $\langle D_{\text{GOS}} \rangle = 2.99 \pm 0.14$ kpc. The parallax distance is more uncertain, $\langle D_{\text{Gaia}} \rangle = 2.47 \pm 0.57$ kpc. For these statistics, we exclude three stars unlikely to be association members (Lee & Lim 2008): HD 15642 and HD 14442 (larger distances) and HD 14633, located at a much different Galactic latitude ($b = -18.20^\circ$).